Reliability Screening of Lower Melting Point Pb-Free Alloys Containing Bi

Joseph M. Juarez, Jr., Michael Robinson, Joel Heebink
Honeywell
AZ, US
mike.robinson6@honeywell.com
joseph.juarez@honeywell.com

Polina Snugovsky, Eva Kosiba, Jeffrey Kennedy, Zohreh Bagheri, Subramaniam Suthakaran, Marianne Romansky
Celestica Inc.
Toronto, ON, Canada
polina@celestica.com

Abstract
This paper is the second of two papers discussing the companies Lower Melt Alloy program. The first paper was presented at IPC APEX2013. The program explores the manufacturability and reliability of three Pb-free Bi-containing alloys in comparison with conventional SAC305 and SnPb assemblies. The first alloy included in the study is a Sn-based alloy with 3.4%Ag and 4.8%Bi, which showed promising results in the National Center for Manufacturing Sciences (NCMS) and German Joint (GJP) projects. The other two alloy variations have reduced Ag content, with and without Cu.

BGA and leaded components were assembled on medium complexity test vehicles using these alloys, as well as SAC305 and SnPb as base line alloys for comparison. Test vehicles were manufactured using two board materials, 170°C glass transition temperature (T_g) and 155°C T_g, with three surface finishes: ENIG, ENEPIG, and OSP. The ATC testing was done at -55°C to 125°C with 30 minute dwells and 10°C/min ramps, and vibration testing at two G-Force test conditions with resistance failure monitoring was performed on the daisy chained components.

In this paper, the results of 3000 ATC cycles are discussed. The paper gives a detailed description of the technique for the vibration testing using 2 and 5 G harmonic dwells. In addition, the results of vibration testing and some preliminary data analysis are discussed. These results provide data for further statistical analysis leading to the choice of proper combinations of the solder alloys, board materials, and surface finishes for high reliability applications.

Introduction
Aerospace and military companies continue to exercise RoHS exemptions and to intensively research the long term attachment reliability of RoHS compliant solders. Their products require higher vibration, drop/shock performance, and combined-environment reliability than the conventional SAC305 alloy provides. The NASA-DoD Lead-Free Electronics Project confirmed that pad cratering is one of the dominant failure modes that occur in various board level reliability tests, especially under dynamic loading [1].
One possible route to improvement of the mechanical and thermo-mechanical properties of solder joints is the use of Pb-free solders with lower process temperatures. Lower temperatures help reduce the possibility of damaging the boards and components, and also may allow for the use of lower T_g board materials which are less prone to pad cratering defects. There are several Sn-Ag-Bi and Sn-Ag-Cu-Bi alloys which melt about 10°C lower than SAC305. The bismuth in these solder compositions not only reduces the melting temperature, but also improves thermo-mechanical behavior [2-4]. An additional benefit of using Bi-containing solder alloys is the possibility to reduce the propensity to whisker growth [5]. Alloys containing Bi have not been widely utilized due to the formation of a low melting ternary SnPbBi alloy when SnAgCuBi solder joints are contaminated with Pb from SnPb component finishes. With the increased use of lead-free solder alloys and component finishes, SnPb component finishes are becoming obsolete, reducing the risk of Pb contamination of Bi-containing solder alloys.

Several ternary SnAgBi and quaternary SnAgCuBi Pb-free solder alloys have shown great mechanical and thermo-mechanical reliability in previously completed projects: National Center for Manufacturing Sciences (NCMS) [6] and JCAA/JGPP Lead-Free Solder Project [7] and new studies (GJP Lead-Free Avionics) recently presented at the Aerospace Industry Association (AIA) PERM meeting [8].

Some of these Pb-free alloys have melting temperatures comparable to SnPb, allowing for the use of SnPb processing temperatures for Pb-free assemblies. Some alloys may have a lower Ag content that will reduce the solder cost and contribute to mechanical property improvements.

Celestica, in a partnership with the University of Toronto, has been working on a project with the objective of selecting new Pb-free alloys with process temperatures comparable to conventional SnPb solder for assembly and rework of ball grid array, leaded, and pin-through-hole components since 2009 [9]. From an initial list of 23 alloys studied for metallurgical performance, a total of seven SnAgBi and SnAgCuBi alloys selected for screening experiments of mechanical and thermo-mechanical properties showed good manufacturability and drop test performance.

This paper is the second of two papers discussing the companies Lower Melt Alloy program. This program explores the manufacturability and reliability screening results for three Bi-containing alloys in comparison with conventional SAC305 and SnPb assemblies. In addition to the results published in the first paper, mostly focused on the manufacturability and metallurgical analysis after solidification and thermal cycling, this paper presents the results of -55 to 125°C ATC after 3000 cycles and vibration testing using 2 and 5 G harmonic dwells. This paper gives a detailed description of the technique for the vibration testing. Some topics such as alloy selection and test vehicle description are repeated in this paper for the reader's convenience.

Experimental

Alloy selection

Three alloys out of seven analyzed in the previous study [9] were selected for the high reliability environment testing. The alloy names, constituent elements, minimum melting temperatures and melting temperature ranges are shown in Table 1.

Table 1: Alloy Selected for High Reliability Screening Experiments

#	Board Name	Alloy Constituents	Alloy Composition	Min Melting Temperatures, °C (Experimental)	Melting Range, °C
1	Paul	SnAgBi	Sn3.4%Ag4.8%Bi	206	11
2	Violet	SnAgCuBi	Sn2.25%Ag0.5%Cu6.0%Bi	205	10
3	Orchid	SnAgBi	Sn2.0%Ag7.0%Bi	190	25
4	SAC305	SnAgCu	Sn3.0%Ag0.5%Cu	217	6
5	SnPb	SnPb	Sn37.0%Pb	183	0

Alloy #1, proposed by Paul Vianco, is labeled "Paul". This alloy's excellent thermomechanical properties for harsh environments have been proven by NCMS [6] and the German Joint Lead-Free Avionics project [8]. Alloys #2 and #3 are modifications of the "Paul" alloy.

Alloy #2 "Violet" has a lower Ag content and does not form Ag_3Sn plates**,** the absence of which may help to improve drop/shock properties. Cu is added to the formulation to reduce the Cu dissolution potential. The optimized Bi content related to the reduced Ag may help to better mitigate whisker formation and to slightly lower the melting temperature compared to the "Paul" alloy. Both alloys have an excellent pasty range.

Alloy #3 "Orchid" is a variant of the "Paul" alloy, with lower Ag and higher Bi content, which allows the significant reduction of the minimum melting temperature. The pasty range is wider than in alloys #1 and #2. Because of a lower melting temperature and higher Bi content, it may dissolve even less Cu and provide greater whisker mitigation than Alloy #1 "Paul".

SAC305 and SnPb solders are included in the test matrix for baseline comparisons. No-clean solder pastes of the experimental alloys were produced by one of the major solder paste suppliers. The solder paste performance evaluation was done using a company test vehicle and a standard company solder paste evaluation procedure [10].

Test vehicle

The test vehicle, designed by Honeywell, has been used for numerous tin-lead baseline and lead-free process development activities. The board stack up and dimensions are representative of a large percentage of aerospace products and designed per IPC-4101/126 and /129 requirements. Assembling this-well characterized board in a variety of board finishes while processing duplicate sets of components should make the comparison of various low melt lead-free alloys easier.

The assembly and reflow processes at the company Process Development Center have been optimized to accommodate the assembly of various daisy chained SAC 305 BGA and matte tin leaded components.

Board materials

The objective of testing different laminate materials is to evaluate the pad cratering benefit obtained when using a lower T_g material enabled by the lower process temperature. This lower T_g in combination with the low melt alloy is expected to deliver equal or better performance at a potentially lower cost point.

Table 2: Laminate Materials

T_g (°C)	Laminate
155	Nelco 4000-7
170	Isola 370HR

Board surface finishes

Multiple surface finishes are used to compare soldering performance at various metallic interfaces and to review reliability performance when soldered to copper or nickel.

Table 3: Surface Finishes

Surface Finish	Supplier	Thickness (µm)
OSP	**Entek 106A**	**n/a Copper Triazole**
ENIG	**MacDermid**	**Ni 3.81 Au 0.13-0.20**
ENEPIG	**Uyemura**	**Ni 3.81 Pd 0.05 Au 0.08**

Dimensions and number of layers

The overall dimensions for the PWB test vehicle are approximately 203 mm x 355 mm and 2.5 mm thick, with 16 layers of alternating copper signal and ground/power planes. All of the wiring on the PWB is to accommodate daisy chain active resistance monitoring and output to an edge connector pattern for wiring. Figure 1 illustrates the test vehicle, which includes packages representative of the variety typically seen on products.

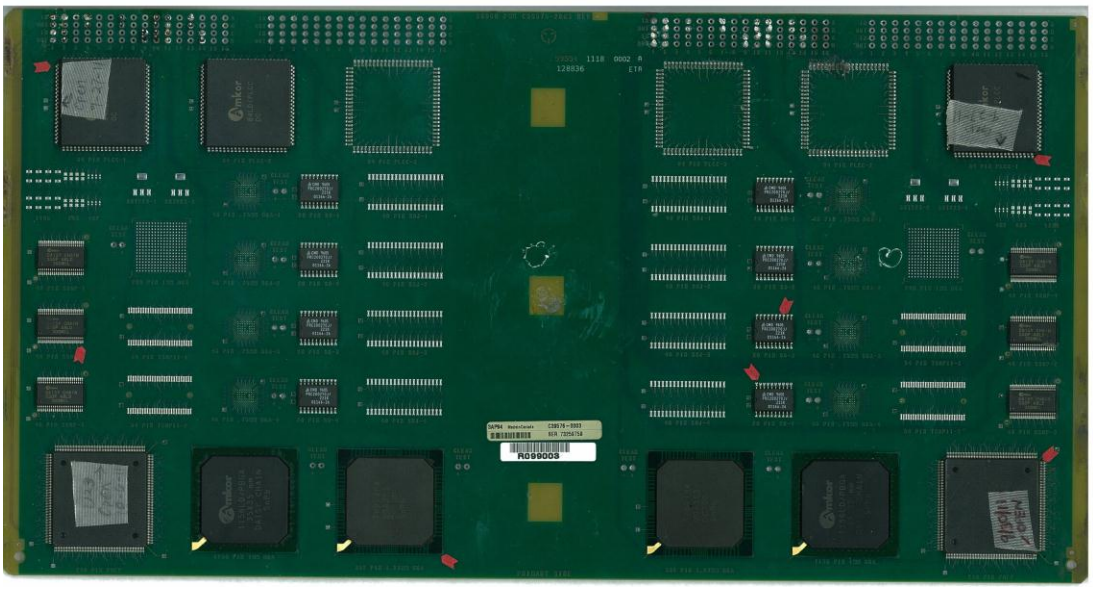

Figure 1: Test Vehicle

The package types, component dimensions, I/O counts, solder ball composition, and lead finishes are shown in Table 4: Component Table 4: Component Types.

Table 4: Component Types

I/O Count/ Package	Dimensions	Pitch	Lead Finish	Ball Composition
20 /SO	**6.35 X 12.70 mm**	**1.27 mm**	**SnPb and Matte Tin**	
40 /SOJ	**10.16 X 25.40 mm**	**1.27 mm**	**SnPb and Matte Tin**	
48 /SOP	**5.08 X 15.24 mm**	**0.50 mm**	**SnPb and Matte Tin**	
54 /TSSOP	**10.16 X 21.59 mm**	**0.64 mm**	**SnPb and Matte Tin**	
84 /PLCC	**29.21 X 29.21 mm**	**1.27 mm**	**SnPb and Matte Tin**	
240/ PQFP	**31.75 X 31.75 mm**	**0.50 mm**	**SnPb and Matte Tin**	
289 /BGA	**17.15 X 17.15 mm**	**1.02 mm**		**SnPb and SAC 305**
352 /BGA	**35.56 X 35.56 mm**	**1.27 mm**		**SnPb and SAC 305**
1156/ BGA	**34.93 X 34.93**	**1.02 mm**		**SnPb and SAC 305**

These partially assembled boards were continuously monitored with resistance event detection equipment during harsh environment accelerated thermal cycling and vibration exposures representative of product requirements. The range of component type, size, and board finishes provide a comprehensive look at selected lower melt Pb-free alloys that can be compared to SAC 305 and SnPb baseline test data.

This screening experiment defines the critical variables and provides a path for more in-depth industry studies of low melt solders, while minimizing the costs.

Assembly

Fifty six of the above test vehicles were built at the company using different combinations of board material, surface finish and alloys as outlined in Table 5.

Table 5: Build Matrix

Board Material	Alloy	Surface Finish		
		ENEPIG	ENIG	OSP
Normal T_g 155 °C	SnPb	2		3
	SAC305	2		2
	Paul			4
	Violet		4	
	Orchid	4		
High T_g 170 °C	SnPb	2		3
	SAC305	2	1	3
	Paul	4	4	
	Violet	4		4
	Orchid		4	4

Seven thermocouples were placed on test vehicle assemblies at various locations, both on components and on the board itself, to determine the optimal profiles. Two profiles were used; one with a peak reflow temperature of 240°C for SAC305 and one with a peak reflow of 222°C for all other alloys. In both cases, the time above liquidus was between 70 and 90 seconds. The profiles are shown in Figure 2 and Figure 3 respectively. All boards were reflowed in a 10-zone production reflow oven.

During the solder screening process, solder paste heights and volumes were measured. Every attempt was made to print equal volumes of the various solder pastes. All components were placed using a production placement machine with a standard nozzle. Visual and X-Ray inspections were then performed on each of the assembled boards. Additionally, one assembly was sent for cross sectioning to ensure the appropriateness of the profiles prior to completion of the build.

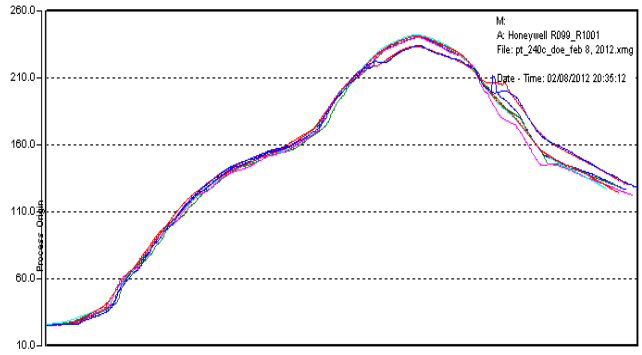

Figure 2: Reflow Profile for 240°C

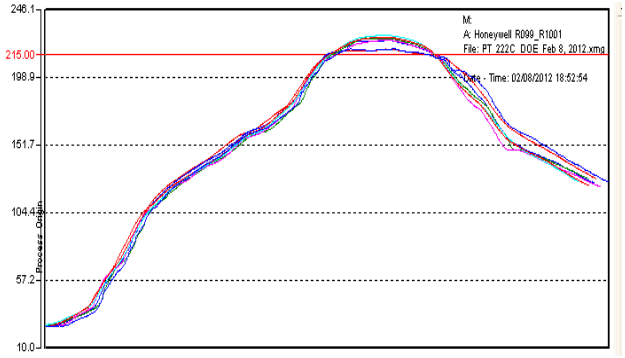

Figure 3: Reflow Profile for 222°C

Accelerated Temperature Cycling

17 test vehicles were exposed to Accelerated Temperature Cycling (ATC). ATC was performed to a target range of -55°C to 125°C with a ramp rate of 10°C/min and a 30 minute dwell at each extreme. Temperature measurements for guiding the profile were measured at the test vehicle level (not the chamber level). The actual profile resulted in a hot dwell at 130°C for 38 minutes and a cold dwell at -58°C for 39 minutes with a 13 minute ramp in between, totaling 103 minutes per cycle as shown in Figure 5. The assemblies were placed into two racks within the chamber, as seen in Figure 4, to allow the air to circulate freely. 3010 cycles were completed before testing was terminated.

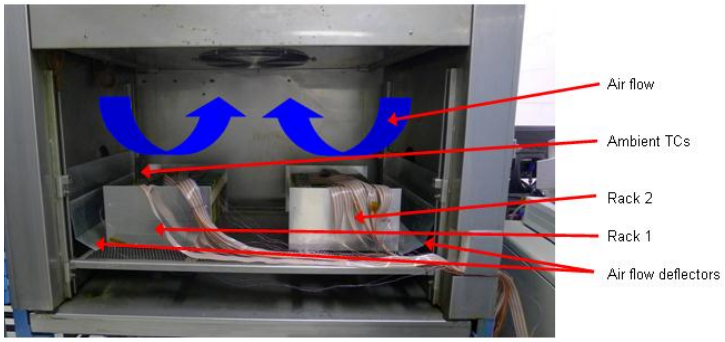

Figure 4: ATC Chamber Set Up

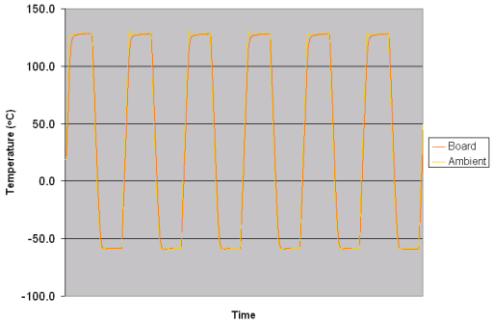

Figure 5: ATC Chamber Profile

Event detectors were used to monitor the resistance thresholds of 32 components on each board. A failure was recorded when the channel resistance increased to 300 W or more for at least 200 ns. Each recorded failure was electrically probed at room temperature to determine the location of failure within the component, or whether it was a board or trace issue or an issue within the cable connection. Selected failed components were cut from the board for detailed analysis, while the remaining components were returned to the chamber for further temperature cycling.

Vibration testing

26 test vehicles were subjected to vibration testing; 17 at a 5G level and 9 at a 2G level. Resistance, strain and vibration data were recorded. Component failure was determined through resistance monitoring using the same method described in the ATC testing section. Strain was monitored at regular intervals throughout the test on a representative sample size of boards. Vibration was monitored using an accelerometer at the center of each board, the area that would experience the most flexure. Figure 6 shows four boards installed in the fixture with the various monitoring systems.

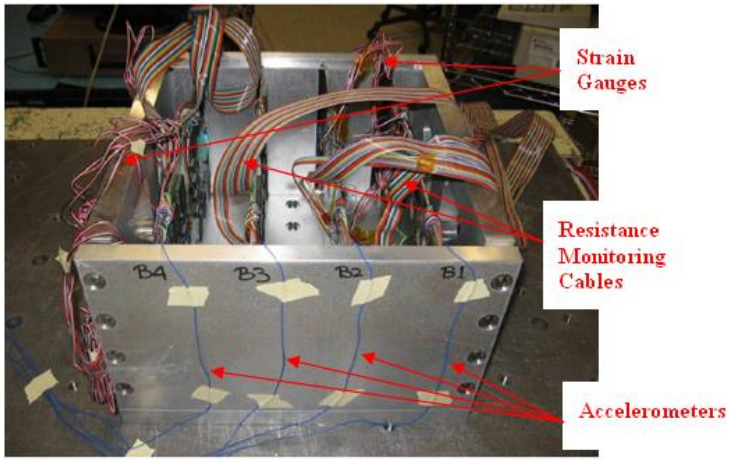

Figure 6: Vibration Fixture with Boards

Boards of the same material and similar finish/alloy combinations were grouped together for testing. A summary of the grouping is shown in Table 6.

Table 6: Vibration Test and T_g / Alloy / Finish Parameters per Group

T_g / Alloy / Finish		Location			
Vibration Level	**Group**	**B1**	**B2**	**B3**	**B4**
5G	1	170 / Violet / ENEPIG*	170 / Paul / ENIG	170 / SAC305 / ENEPIG	170 / SnPb / ENEPIG
	2	170 / Paul / ENEPIG**	170 / SnPb / OSP		
	3	170 / Orchid / ENIG*	170 / Violet / OSP	170 / SAC305 / OSP	170 / Orchid / OSP*
	4	155 / Orchid / ENIG*	155 / SAC305 / OSP	155 / SnPb / OSP	
	5	155 / Violet / ENIG**	155 / SAC305 / ENEPIG	155 / SnPb / ENEPIG	155 / Orchid / ENEPIG**
2G	6	155 / Paul / OSP	155 / Violet / ENIG	155 / Orchid / ENEPIG	
	7	170 / Paul / ENIG	170 / Violet / ENEPIG	170 / Orchid / OSP	
	8	170 / Paul / ENEPIG	170 / Violet / OSP	170 / Orchid / ENIG	

*Strain gauge scenario 1 was used as seen in Figure 7. ** Strain gauge scenario 2 was used as seen in Figure 8.

Since only boards which were used for 5G testing had strain gauges attached, these boards were exposed to sine sweeps at both 2G and 5G to characterize the boards. The boards used for 2G testing were only exposed to a 2G sine sweep to determine the appropriate resonant frequencies. After the sine sweeps, the group of boards was then exposed to approximately 6 hours of sine dwell at the assigned vibration levels.

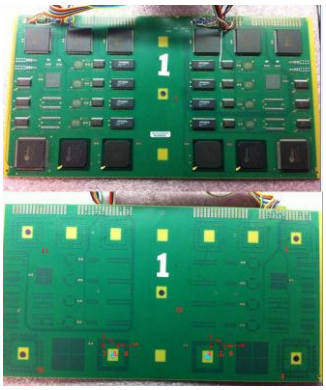

Figure 7: Vibration Strain Gauge Location Scenario 1 (showing both front and back of board)

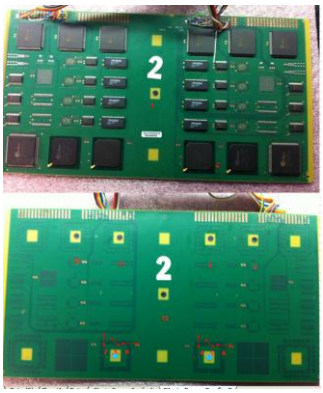

Figure 8: Vibration Strain Gauge Location Scenario 2 (showing both front and back of board)

The 26 allocated cards were divided into 8 testing groups. The first 5 groups were assigned to 2G and 5G sweeps and a 5G dwell; the remaining 3 groups were assigned to 2G and 5G sweeps and a 2G dwell.

An aluminum fixture was built to hold a maximum of four cards. The fixture has 8 wedge locks with special locking mechanisms to secure the cards. The wedge locks were used to lock the test sample by grabbing the shorter opposing edges of the sample and ensured samples did not touch the base of the fixture. The wedge locks were all torqued to 8 lb-in at the start of the test. A fixture survey was completed on the vibration table using sensors to make sure there was no fixture resonance in the test frequency range.

A 12000 pounds force capacity electrodynamics shaker with a Spectral controller was used for the vibration testing. The input control accelerometer was mounted on the fixture. During vibration testing, each board's response acceleration level was monitored using an accelerometer attached to the middle of the boards. In addition, strain gauges were mounted at strategic locations selected on the assembly to provide data for the strains experienced by components of interest. This combination of data from acceleration sensors, the various strain gauges, and active monitoring of the resistance of the daisy chain components provided the base data for analysis of the vibration performance of the assembly.

Each card group included a different combination of alloys, finishes and laminate T_g. Each group went through a 2G sweep and a 5G sweep to find the resonance frequency of each test vehicle. Then the dwell frequency of each batch was determined based on the best closest frequency of each test vehicle resonance frequency, causing roughly equal deflection in all test vehicles of that batch. The overall observed resonance frequency range of the 26 boards was 48 – 60 Hz. The card G level range for the first 5 groups vibrated at a 5G peak was 45 - 65G. Further investigation revealed that groups 3 and 5 were observed at slightly higher resonance frequencies and as a result, slightly higher card G levels. Cross section analysis was performed on one test vehicle after the vibration test and there were no cracks found between the layers of the raw test vehicle, therefore, this resonance frequency shift for these two groups is related to material properties of these groups' boards. It was not possible to further narrow down the cause any of the shifts due to the number of variables. In the beginning of the sine dwell vibration, the card deflections were observed by eye to be similar, and confirmed by strain readings at strain gauge locations 1 and 12, which were at the middle of the board; strain gauge 1 was on the top side and 12 was on the bottom side. These readings in the middle of the boards where maximum deflection occurs were fairly consistent across all 4 boards in the fixture. This suggests that the deflections are comparable. It is apparent by the collected data that the cards in group 3 bent less than all other groups as the G level here was greater than the rest; this might suggest these test vehicles are stronger. As stated earlier, the lesser deflection of the group 3 cards related to properties of materials of these cards due to alloy type or lamination type or surface finish. Strain gauges were attached to one card of each group of the first five groups.

The Strain Measurement System was used to measure the strain level of strain gauged boards. When assigning strain gauge locations, we considered that achieving a rough understanding of the strain level in each component was needed. There were two configurations of strain monitoring which included two rosettes (3 axis) and six single axis strain gauges attached to each board. By using two configurations, we were able to maximize the use of our strain system and monitor a larger group of components and assembly locations. Two single axis strain gauges were both vertically and horizontally centered on the front and back of the boards; these locations were used as universal points considering that maximum strain occurs here. Two rosette strain gauges were attached directly under the two BGA components closest to the horizontal center, and the other four strain gauges were placed under QFPs and PLCC84s. Reference Figures 6 and 7 for diagrams of these configurations.

During the sine sweep vibration for all groups, strain monitoring was performed throughout. This data was used to validate the setup and to confirm the maximum strain occurring at the resonance frequency, whereas strain monitoring only occurred for the first five minutes of each hour of the sine dwell. The scan rate was 200 data points per second. When resonance was achieved, maximum strain occurred in the center of the board where the range was roughly 200 - 240 micro strain for the 5G Sweep. This suggests that the maximum deflections of all batches were very similar. Also it has been noted that the group 3 strain values were at the lower end of this strain range, which reinforces our earlier finding of lower deflection due to material properties of this group of boards.

Only sixteen daisy chained components on all cards were resistance monitored during test using an event detector to collect real time electrical failure data. The data collection rate was two seconds and the cycle time was twenty seconds; therefore, ten data points were recorded during every cycle. The resistance was measured across all components all the time. Every two seconds, the system compared the collected value to the threshold value of 300 Ω.

If the measured resistance was greater than the threshold, this reading was considered a failure. If there is a solder or cable break, the system also evaluates this as a fail, therefore, strain relief using clear tape to secure the cable to the fixture was employed, as shown in Figure 11.

Test Procedure and Techniques

Fixture Survey

A sine sweep fixture survey to ensure no resonance occurred within the test frequency range was conducted as seen in Figure 9. The accelerometer closest to the table was chosen as the control accelerometer. The other six accelerometers (five visible, one hidden behind the fixture) were used as auxiliary accelerometers to monitor the response of the fixture during the survey. These auxiliary accelerometers are labeled channels 3 through 8 on the data plot. See Figure 9 and Figure 10 for the fixture sweep set up and resulting data plots.

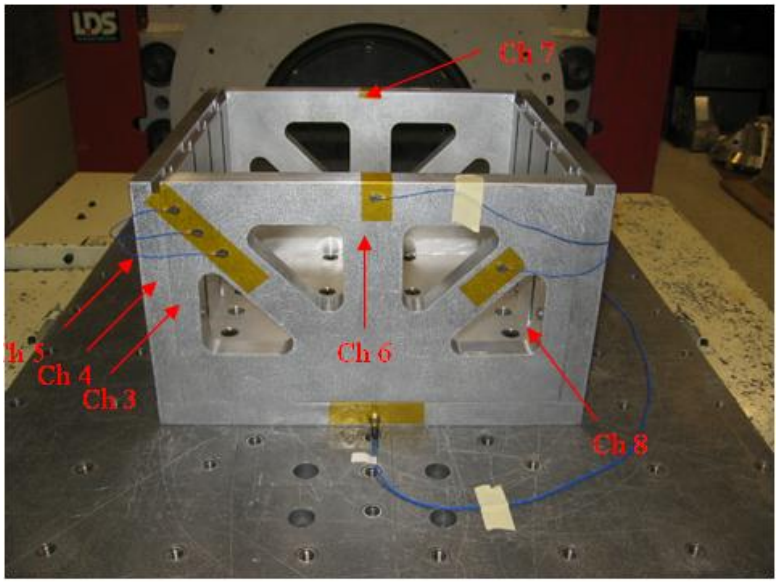

Figure 9: Fixture Sweep Setup

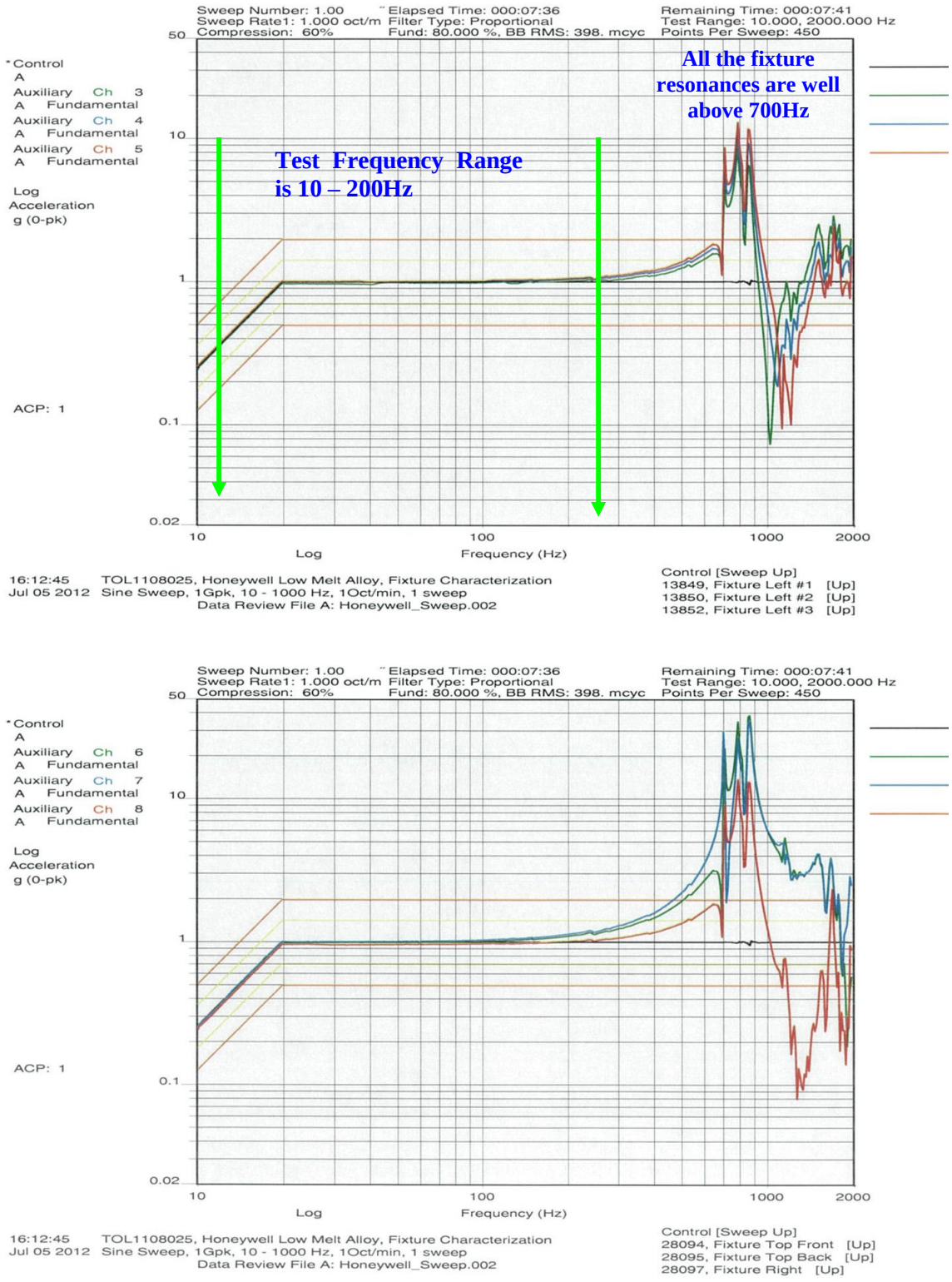

Figure 10: Fixture Sweep Data Plots

The fixture resonance as shown in the Figure 10 graph occurs above 700 Hz; this is well above the testing frequency of 10 - 200 Hz and provides enough guard bands so that the fixture will not be a factor in the assembly performance results, where the card resonance occurred in the range of 45 – 68 Hz.

Vibration Testing

Sine sweep vibration was performed from 10 - 200 Hz at levels of 2G and 5G for each group to find the resonance frequencies of the boards. Following the sweeps, each batch was subjected to sine dwell vibration for 6 hours at the closest common resonance frequency. The response G level on each board was measured.

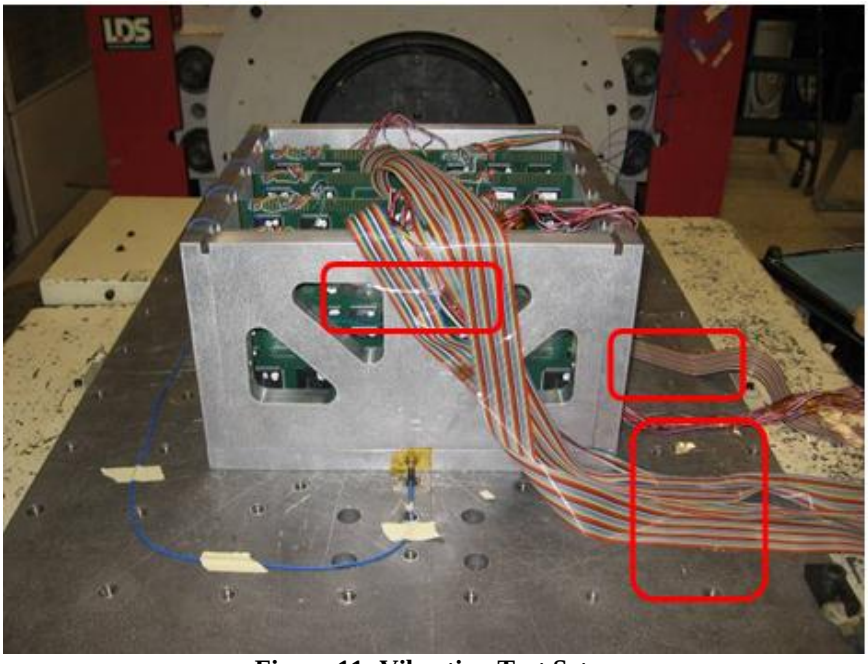

Figure 11: Vibration Test Set up

Strain Monitoring

There were two configurations of strain gauge attachments, where 2 rosettes and 6 single axis strain gauges were attached to each board. For each test, 12 channels were monitored using the Measurement System. Strain measurements were taken for all 2G and 5G sweeps. Strain measurements were recorded only for the first 5 minutes of every hour during the 6 hour dwell. Figure 12 displays how the strain gauges were attached on the test sample. Figure 13 illustrates the first configurations. Figure 14 illustrates the second configuration.

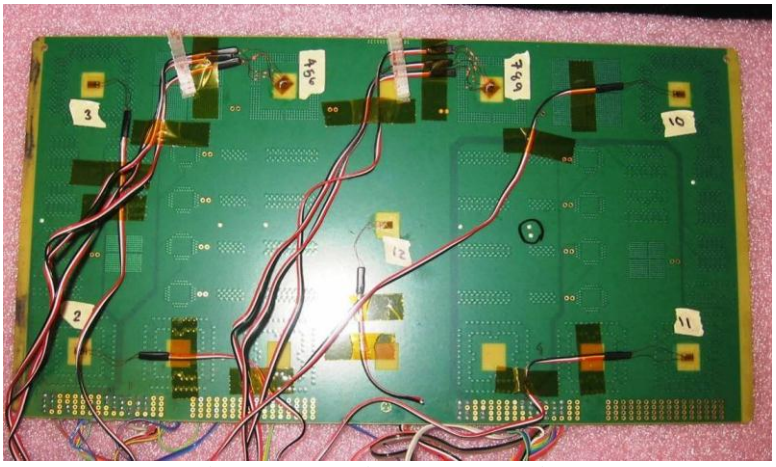

Figure 12: Strain Gauge Locations

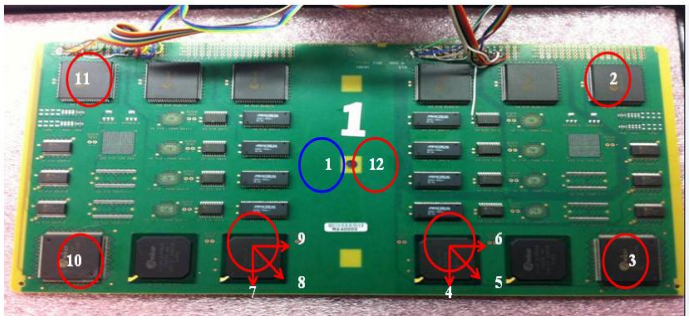

Figure 13: Batch 1, 3, and 4) Blue indicates strain gauge on top side, Red indicates strain gauge on bottom side

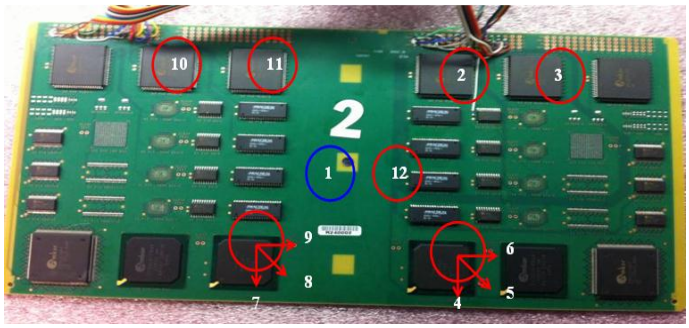

Figure 14: Batch 2 and 5) Blue indicates SG on top side, Red indicates SG on bottom side

The first mode deflection was anticipated from the sine sweep and dwell testing; uniaxial strain gauges were used on most of the component locations. Rosette strain gauges were used on the BGA locations to confirm there was no other directional strain on the test sample.

Resistance Monitoring

All 26 test vehicles were resistance monitored, and 16 components were monitored on each test vehicle. Individual components were each assigned one channel in the resistance monitoring system. For example: four test vehicles were in one batch, and 64 channels were monitored. The event detector data collection was set up with a cycle time of 20 seconds, a data collection rate of every 2 seconds, and the data collection duration was the full testing time. Every two seconds, the system compared the collected value to the threshold value of 300 Ω. If the measured resistance was greater than the threshold, it was considered a failure. Figure 15 displays the resistance monitoring system set-up.

Figure 15: Resistance Monitoring System Set Up

Results and Discussion

ATC reliability test results and analysis

A total of 3010 cycles of ATC were completed. Periodically, the chamber was stopped and the failures recorded by the event detector were removed and verified by manual resistance measurement. If the failure was determined to be within the component, as opposed to the cabling system or a trace failure within the board, the component was cut out for future failure analysis before the test vehicle was returned to the chamber and testing resumed.

It was shown in the previous paper that there were no solder joint failures on either high or normal T_g boards after 1548 cycles at -55°C to 125°C [11]. However, there were via failures in normal T_g boards with OSP finish, assembled using SAC305, Sn3.4Ag4.8Bi (Paul), and SnPb solders. Of these via failures on normal T_g OSP finished boards, only the SAC305 cell did not meet the aerospace qualification requirement of 1000 cycles.

Between 1548 and 3010 cycles, only 3 failures were recorded. These included one BGA built using SnPb solder and SnPb solder balls (1734 cycles) and two BGAs built using Violet solder paste and SAC305 solder balls (2076 cycles and 2466 cycles), all on an OSP finish. Cross-sectioning revealed board failure due to barrel cracks through the via, as seen in Figure 16. Almost-complete cracks were found in the SnPb BGA solder joint (Figure 17: SnPb on OSP). Only partial cracks were formed in the Violet BGA (Figure 18); the electrical failures in this case are attributable to barrel cracks found within the board materials, specifically cracking of the vias.

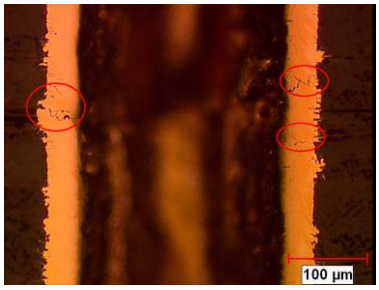

Figure 16: Via beneath BGA SnPb on OSP

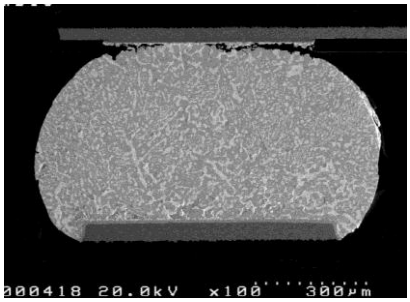

Figure 17: SnPb on OSP

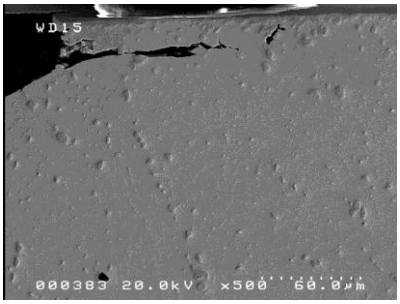

Figure 18: Violet on OSP

Further examination of the microstructural changes that occurred during ATC can best be done on the QFPs, where the solder joint composition is that of the solder paste, as opposed to the BGAs where the solder joint is a combination of the solder paste and the SAC305 solder ball. While no electrical failures were recorded on QFPs with any of the solders tested, cross-sections were prepared for this analysis.

Figure 19 and Figure 20 show the microstructure changes that were observed in the SnPb alloy solder joints. A significant degree of recrystallization and grain growth occurs during the ATC process, resulting in much larger grains and a much larger IMC attach layer. Crack propagation was observed between the grains; in the case of eutectic SnPb between the phases as well as along the intermetallic (IMC). Figure 20 also shows significant pooling of the Pb phase at the IMC layer. As the Pb layer is brittle, this may provide a location for crack propagation.

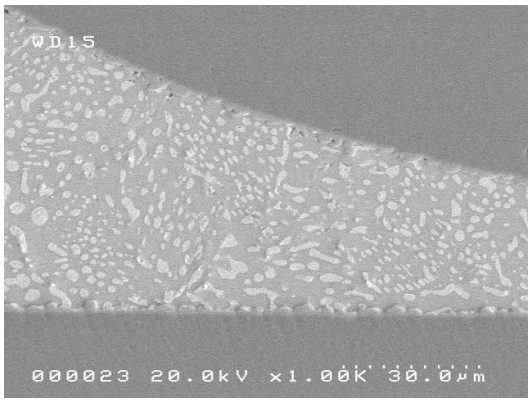

Figure 19: SnPb at Time 0

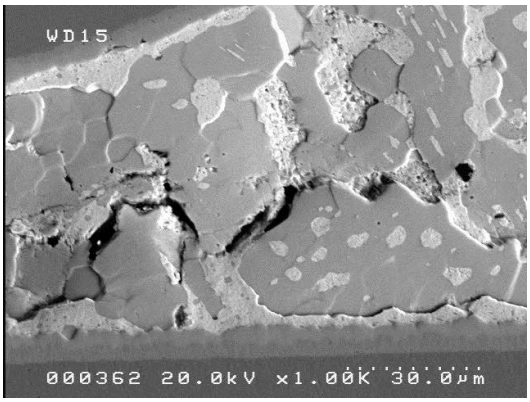

Figure 20: SnPb after ATC

From Figure 21 and Figure 22 one can see the transformation of the SAC305 solder joint between the initial condition and after 3010 cycles. The grains at time zero appear to be surrounded by Ag_3Sn particles and appear significantly smaller than the grains visible after ATC. Also after ATC, the Ag_3Sn particles appear to have coalesced into fewer, larger particles. Additionally, the IMC layers formed between the lead and solder as well as between the solder and copper pad have increased in size and appear to have two phases, Cu_3Sn and Cu_6Sn_5 as seen in Figure 22. A Cu_3Sn layer did not appear to be significant at time zero.

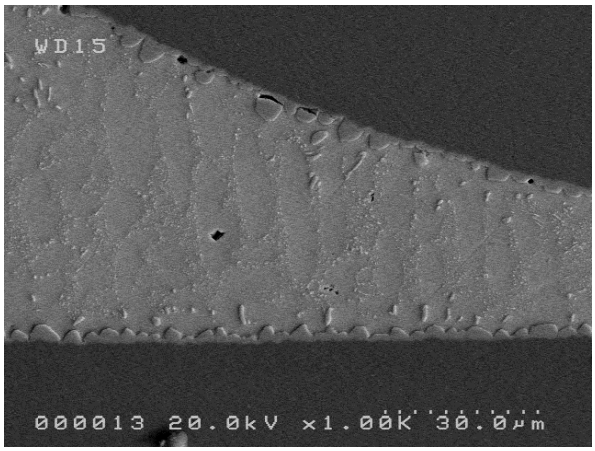

Figure 21: SAC305 at Time 0

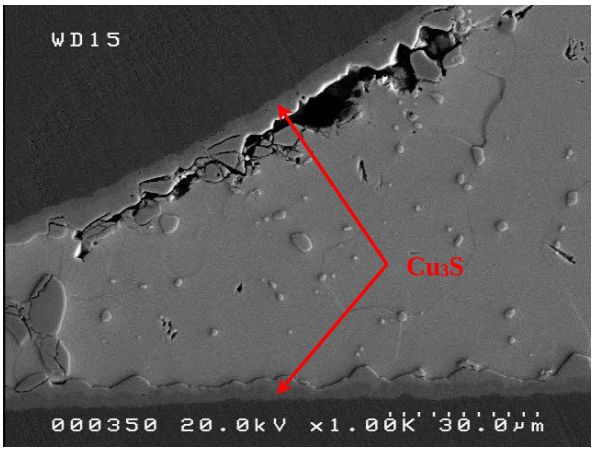

Figure 22: SAC305 after ATC

The Bi-containing alloy called Paul seen in Figure 23 and Figure 24, with approximately 4.8% Bi, showed grain coarsening and IMC growth similar to that seen in SAC305, although the grain growth did not appear to be as dramatic as seen in SAC305.

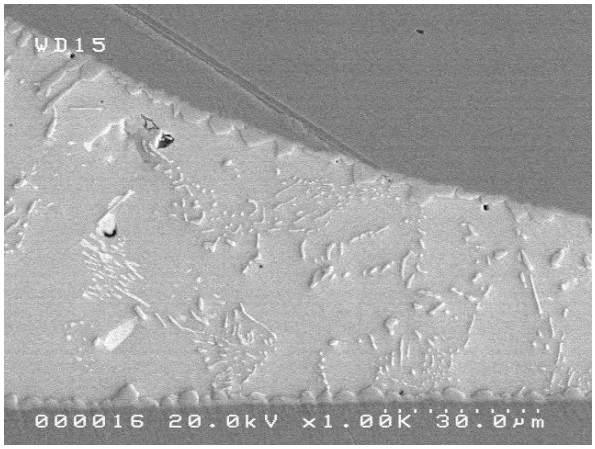

Figure 23: Paul at Time 0

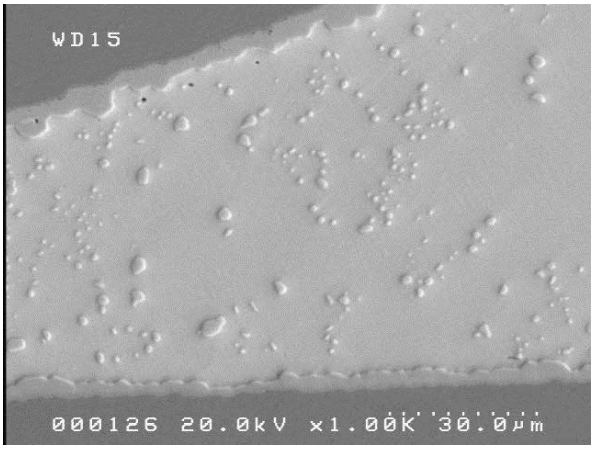

Figure 24: Paul after ATC

The other Bi-containing alloys, Violet and Orchid, contain 6 and 7% Bi respectively. This amount of bismuth appears to have impacted the microstructure in a significantly different manner during ATC. While the IMC layer grew in a similar fashion to the other alloys, the grains do not appear to have coarsened, as seen in Figure 26 and Figure 28. Additionally, the Bi which had previously been present largely in solid solution with Sn (Figure 25 and Figure 27), appears to have been largely precipitated out of the solid solution. This Bi appears to be randomly distributed throughout the solder joint and has not settled preferentially at the IMC layer in the same manner as Pb does in the SnPb alloy.

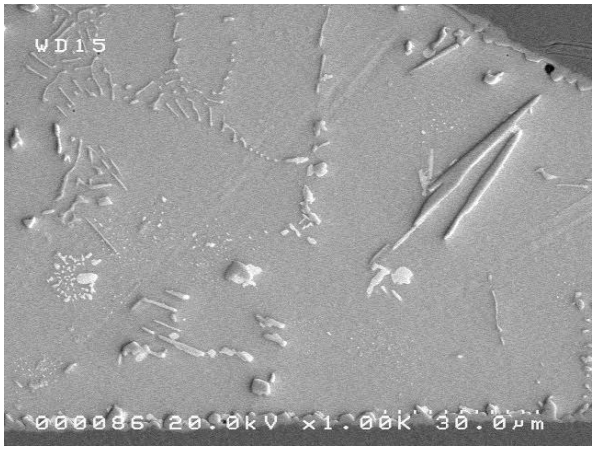

Figure 25: Violet at Time 0

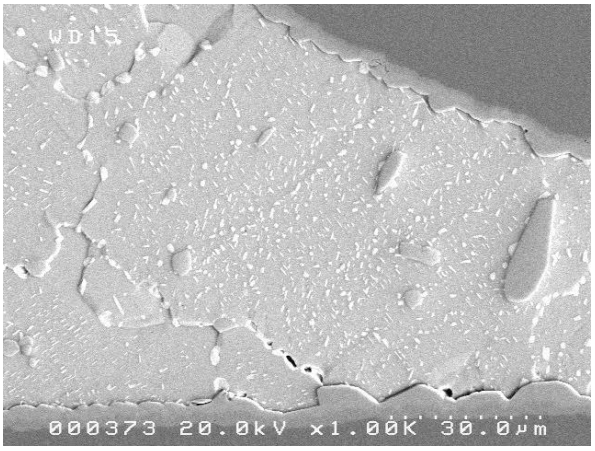

Figure 26: Violet after ATC

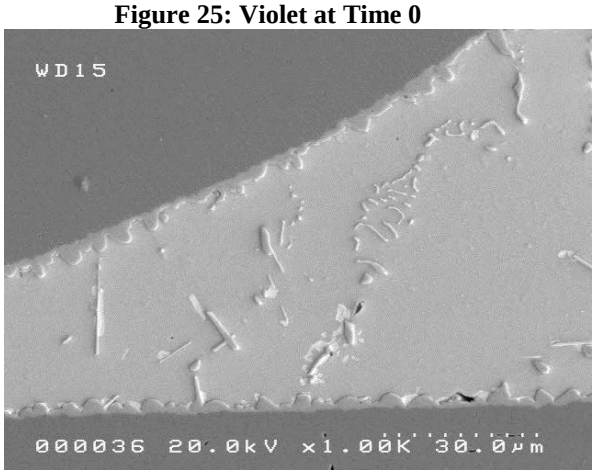

Figure 27: Orchid at Time Zero

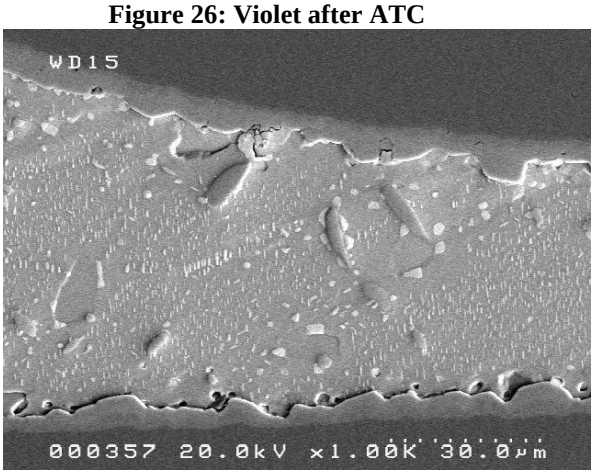

Figure 28: Orchid after ATC

In SAC305 and Paul solder joints, cracks have begun to propagate primarily along the lead-side IMC as seen in Figure 29 and Figure 30: Paul after ATC (QFP crack formation) although none was significant enough to lead to an electrical failure. This type of crack propagation was not seen in the alloys with higher Bi content, Violet and Orchid, as shown in Figure 31 and Figure 32.

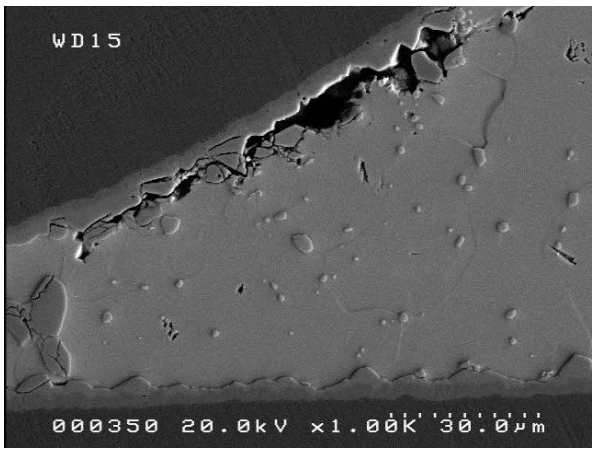

Figure 29: SAC305 after ATC (QFP crack formation)

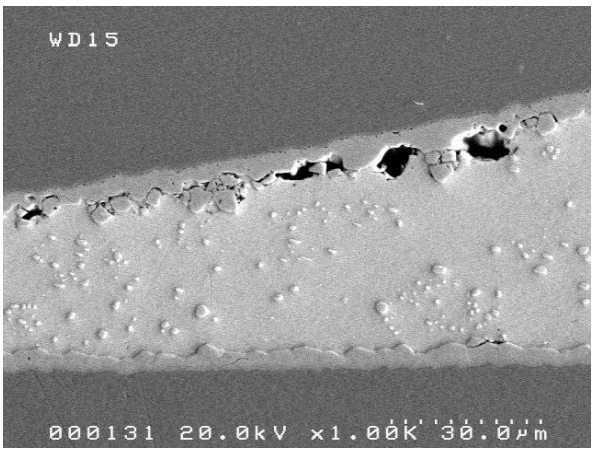

Figure 30: Paul after ATC (QFP crack formation)

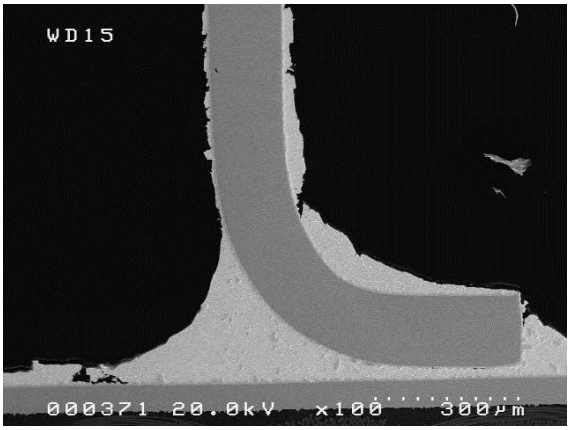

Figure 31: Violet after ATC (no major crack)

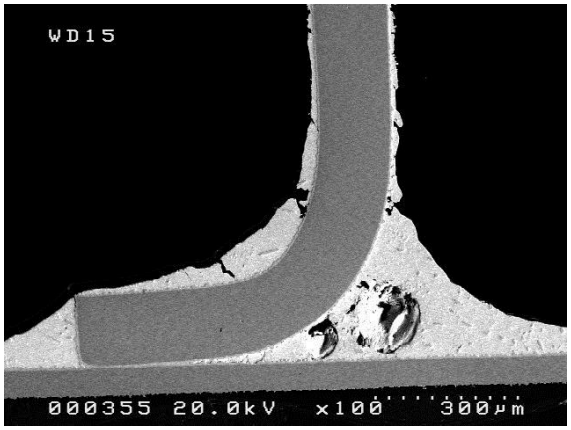

Figure 32: Orchid after ATC (no major crack)

Technique for Vibration Testing Using 2 and 5 G Harmonic Dwells –
Vibration Testing

Sine sweeps revealed that for all these samples, the 1st mode average resonance frequency was 52 Hz. The response accelerometer which was attached on the geometrical center of the board had an average G level at resonance of 55G at an input G level of 5G. Therefore, the average transmissibility, the ratio between input and output, was 10.5. The sine sweep graph below illustrates the test vehicles' response acceleration at their resonance frequencies. The resonance amplitude in displacement was 0.4 inches peak to peak, and due to this high displacement, the board experienced a large bending momentum which led to component solder failure. For the 5G and 2G sweeps, the average test vehicle G level at resonance frequencies were 54.78G and 35.48G respectively. Test vehicle response G levels were measured only at the beginning. The G level deviations during the dwell were not measured. The frequency was held constant throughout the test. The groups 6, 7 and 8 were assigned to the 2G dwell, and the decision was taken not to attach the strain gauges since we didn't expect many failures from the 2G dwell. The test results are shown in Table 7.

As expected, more failures happened during the first two hours of sine dwell testing at the 5G peak, and this failure pattern was noted on all 5G testing. Specifically the BGAs, populated closer to the center of the test samples and experiencing high deflection, failed within first two hours of dwell testing. The strain level distribution on the test samples was high at the beginning of the dwell and there was a significant drop in strain levels roughly after two hours of testing. The noted drop in strain level validated the early stage BGA failures.

Typical 5G Sweep

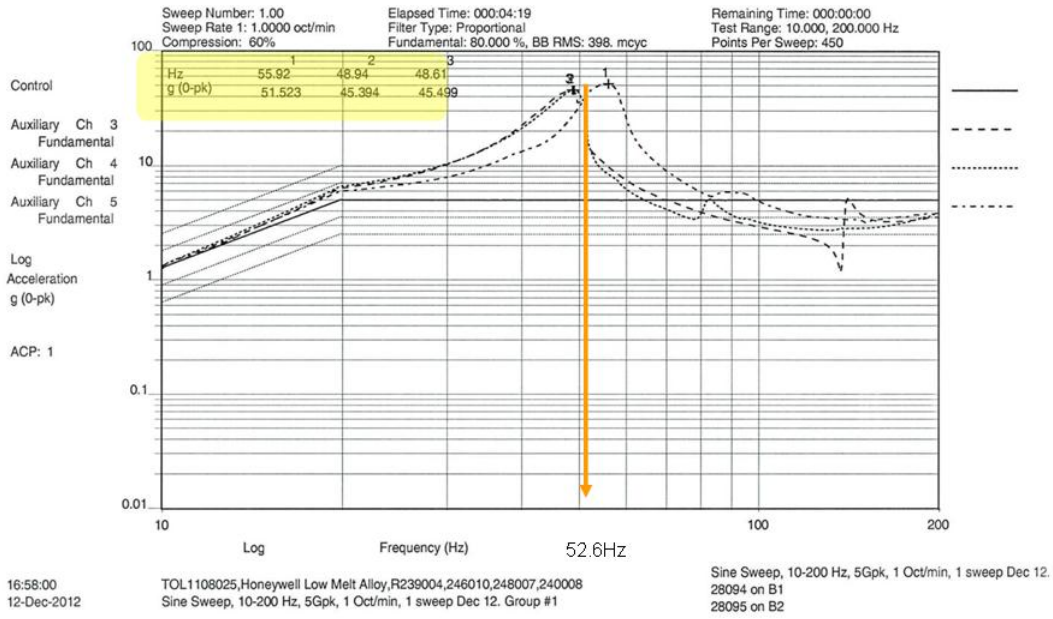

Figure 33: In this batch testing the resonance frequency was 52.6Hz. This is the frequency where individual card response plots intersect and cause almost equal amount of deflection on all cards.

Table 7: Vibration Test Result Summary, 5G and 2G.

Batch Number	Cards	Slot	Tg	Alloy	Finish	Control G Level	Resonance Frequency	Card G Level	Dwell Freq.	Strain Gauge 1		Strain Gauge 12	
										Max [με]	Min [με]	Max [με]	Min [με]
1	R246010	B1	170	B	ENEPIG	5G	48.81 Hz	45.499	52.66 Hz	236	-251	317	-181
	R239004	B2	170	A	ENEG		48.94 Hz	45.394					
	R248007	B3	170	SAC305	ENEPIG		55.92 Hz	51.523					
	R240008	B4	170	Sn-Pb	ENEPIG		55.92 Hz	56.364					
2	R239009	B1	170	A	ENEPIG	5G	-	-	54.81 Hz	218	-213	359	-114
	R240002	B2	170	Sn-Pb	OSP		55.55 Hz	50.350					
3	R247007	B1	170	C	ENEG	5G	62.22 Hz	63.387	60.99 Hz	178	-181	207	-114
	R246002	B2	170	B	OSP		55.92 Hz	59.704					
	R248002	B3	170	SAC305	OSP		60.18 Hz	66.069					
	R247002	B4	170	C	OSP		60.99 Hz	67.143					
4	R239008	B1	155	A	OSP	5G	53.02 Hz	44.566	52.66 Hz	243	-258	262	-242
	R248005	B2	155	SAC305	OSP		52.66 Hz	46.666					
	R240006	B3	155	Sn-Pb	OSP		49.59 Hz	50.816					
5	R246006	B1	155	B	ENEG	5G	54.45 Hz	51.286	56.30 Hz	243	-254	282	-291
	R248009	B2	155	SAC305	ENEPIG		57.05 Hz	59.704					
	R240010	B3	155	Sn-Pb	ENEPIG		56.67 Hz	63.533					
	R247010	B4	155	C	ENEPIG		52.66 Hz	54.450					
6	R239006	B1	155	A	OSP	2G	57.82 Hz	41.687	57.82 Hz	NO STRAIN			
	R246008	B2	155	B	ENEG		47.97 Hz	28.973					
	R247011	B3	155	C	ENEPIG		59.38 Hz	52.966					
7	R239003	B1	170	A	ENEG	2G	57.43 Hz	30.620	56.67 Hz	NO STRAIN			
	R246011	B2	170	B	ENEPIG		48.81 Hz	25.645					
	R247004	B3	170	C	OSP		58.99 Hz	36.308					
8	R239010	B1	170	A	ENEPIG	2G	48.94 Hz	31.915	48.94 Hz	NO STRAIN			
	R246001	B2	170	B	OSP		54.45 Hz	38.282					
	R247008	B3	170	C	ENEG		49.59 Hz	32.961					

In Table 7, the maximum strains on the component side of the test vehicle measured with strain gauge 1 compared to the maximum strains measured on the opposite side with strain gauge 12 are consistently lower due in part to the slight shift of the neutral axis toward the component side. Theoretically the compressive strains should be close to the tensile strains and are close for strain gauge 1, but in the strain gauge 12 measurements only batches 4 and 5 are close. The strain gauge numbering corresponds to the channel numbering shown in Table 8.

Strain Testing

The strain raw data for each testing batch was extracted from the strain system and processed in a software spreadsheet, then the strain versus time graphs were created for each strain gauge location. The strain graphs were used to find the strain distribution on the strain gauged board during sine sweep and dwell. That gave us a better understanding of how the board behaves during the test and gives us a good picture of strain levels of each component during the test. The test results confirmed that the maximum strain happens at the resonance frequency of the card. Then the maximum strain value of each location was determined and is listed in Table 8. The linear strain gauges measure the strain in one direction and the maximum value calculations for linear strain gauges are straightforward. The rosette strain gauges measure the strain in three directions, where two readings are in orthogonal directions and the third one is 45 degrees to the other two and the maximum and minimum principal strains are calculated using those three readings.

Maximum strain occurs at the center of the board and strain values decreased with a non-linear pattern when the strain measurement point moves away from the center. These strain distribution results confirm that the cards resonated at their first mode natural frequency. We found this strain distribution result is similar to the NASA DoD Pb-free project strain distribution results. [12, 13]

A general strain value behavior noted was that the strain value was at its maximum when the dwell started, then it decreased with dwell time. The cards' deflections are high at the beginning of the dwell, since the dwell frequency is very close to the cards' resonance frequency at that stage. The formation and accumulation of laminate and / or solder defects is changing the stiffness, therefore changing the resonance of the test sample. The dwell frequency was maintained consistent throughout the 6 hour dwell, so the card deflection must have decreased over the dwell time and resulted in a decrease in strain as seen in Figure 35.

As Figure 36 indicates, all components' strain values follow a steep downward pattern from the start of the test to just before the two hour mark. From this point forward, strain values appear to remain fairly consistent on a flat line.

Table 8: Maximum Strain Values at 5Gpk Sine Sweep

	Strain Gauges and their Channel numbers									
	CH1	CH2	CH3	CH(4, 5, 6)		CH(7, 8, 9)		CH10	CH11	CH12
	Max(με)	Max(με)	Max(με)	Max(με)	Min(με)	Max(με)	Min(με)	Max(με)	Max(με)	Max(με)
Batch1	236	176	168	146	-66	135	-50	152	120	317
Batch2	218	108	37	87	-73	94	-78	82	127	359
Batch3	178	111	187	117	-46	106	-60	157	123	207
Batch4	243	136	0	92	-79	103	-98	-14	81	262
Batch5	243	134	61	103	-96	123	-96	75	161	282

Strain Distribution on the Samples at Resonance Frequency

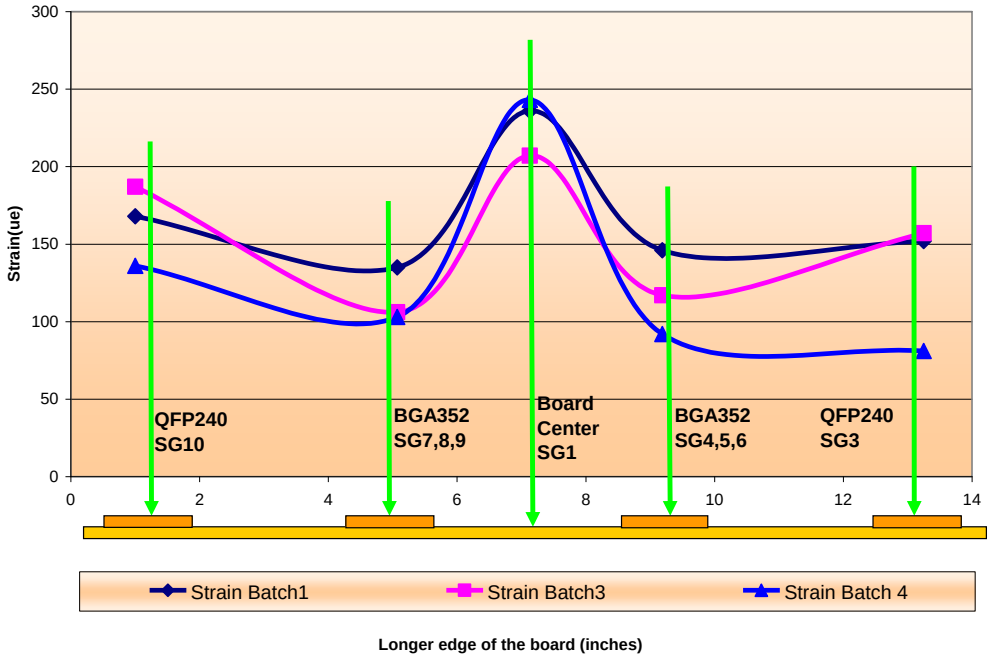

Figure 34: Strain Distribution along Longer Edge of Board

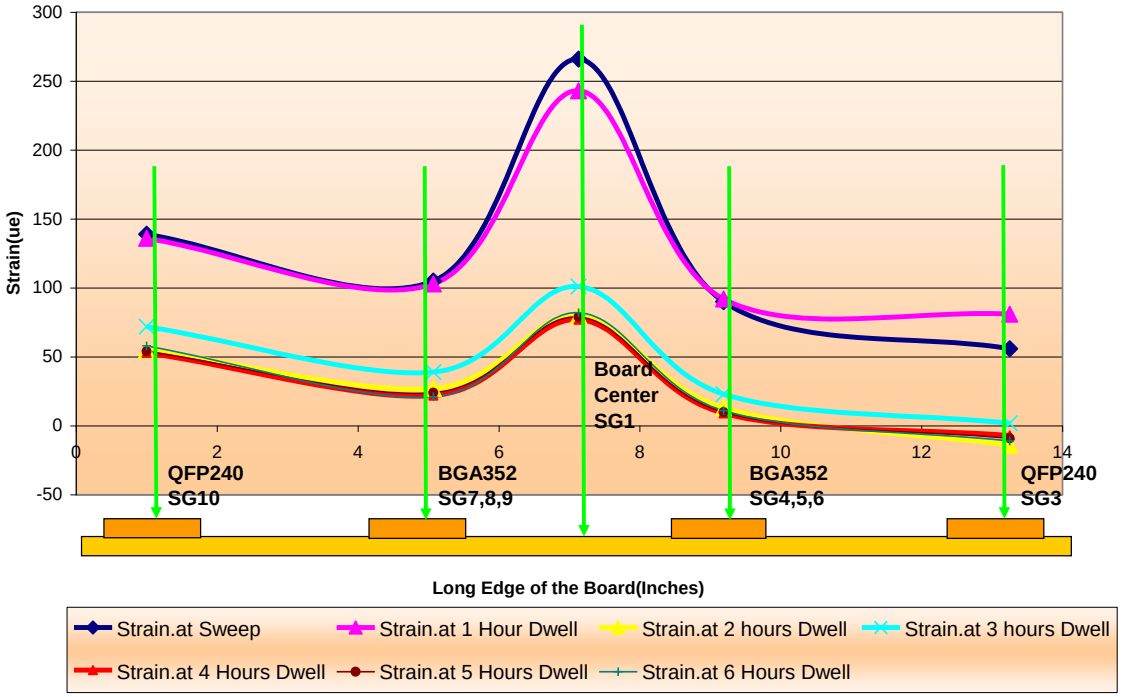

Figure 35: Strain Distribution Change on Components during 6 Hours Dwell

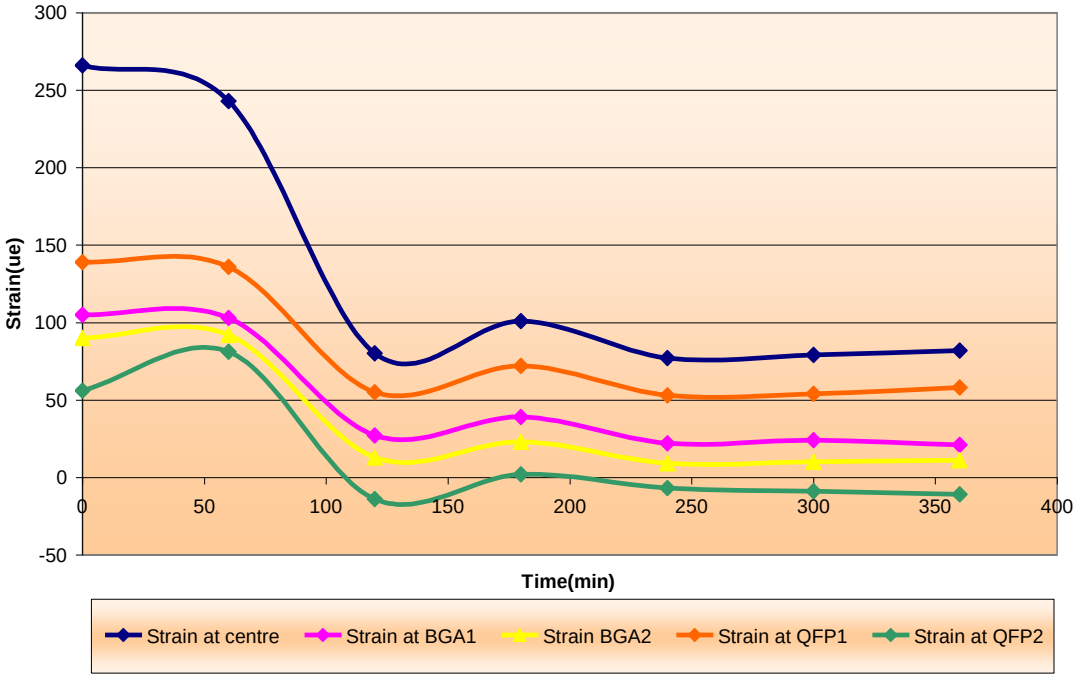

Figure 36: Typical Strain versus Time Graph during Sine Sweep on Components

The strain graphs indicate that the strain level of the sample increased with the frequency during the sweep and reached the maximum when the card experienced the resonance frequency. Strain gauge 1 location is at the component side center of the test sample and strain gauge 12 location is at the bottom side center of the test vehicle; theoretically these locations' strain readings should be equal if the conditions on both sides of the board are the same. In our instance, channel 12 on the bottom of the board displays a slightly higher strain than channel 1 on the component side due to the fact that the components provide local stiffening in their respective regions and as a result create a global stiffening effect on the component side of the card. The testing revealed that the theoretical expectation is correct and the testing methodology is correct.

Figure 37 shows the 5G sweep strain data for channel 1. The test frequency range is 10 - 200 Hz at a rate of 1 octave/min and total duration of 4.18 minutes. As the vibration begins, the test vehicle deflection starts to increase, and that causes the strain to increase. Due to this proportional relationship between strain and displacement, both increased to a maximum value until the resonance frequency occurred at 48.61 Hz, which happened 136.9 seconds from the sweep start. The entire sweep strain data was collected, but the strain graph was plotted only for 2.67 minutes since no valuable strain event occurred beyond this point.

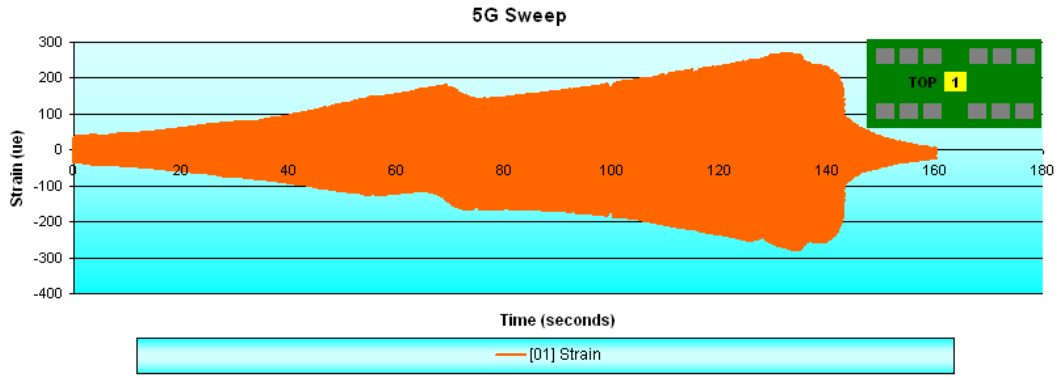

Figure 37: Strain at 5G Sine Sweep on Channel 1

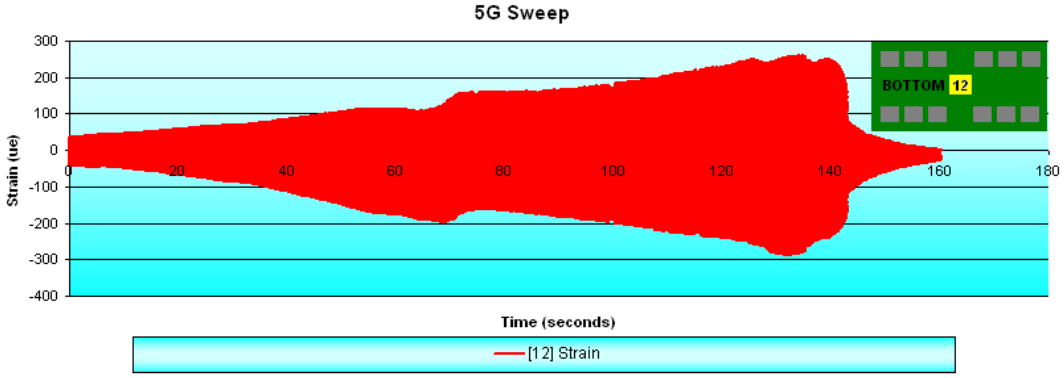

Figure 38: Strain at 5G Sine Sweep on Channel 12

Vibration Resistance Measurement Details

Table 9: Resistance Monitoring Failure Details for 5G test

Card #	R239008	R239004	R239009	R246002	R246006	R246010	R247002	R247007	R247010
Paste type	Paul			Violet			Orchid		
Finish	OSP	ENIG	ENEPIG	OSP	ENIG	ENEPIG	OSP	ENIG	ENEPIG
T_g	155	170	170	170	155	170	170	170	155
352 BGA	02/02	02/02	01/02	00/02	02/02	02/02	02/02	02/02	01/02
240 QFP	02/02	02/02	02/02	00/02	02/02	02/02	02/02	02/02	02/02
SSOP 48	00/06	02/06	00/06	00/06	00/06	00/06	01/06	02/06	00/06
PLCC 84	01/06	04/06	00/06	00/06	01/06	05/06	01/06	02/06	04/06

Card #	R248005	R248002	R248009	R248007	R240006	R240002	R240010	R240008
Paste type	SAC305				SnPb			
Finish	OSP	OSP	ENEPIG	ENEPIG	OSP	OSP	ENEPIG	ENEPIG
T_g	155	170	155	170	155	170	155	170
352 BGA	02/02	02/02	02/02	02/02	00/02	02/02	00/02	02/02
240 QFP	02/02	02/02	02/02	02/02	00/02	02/02	02/02	02/02
SSOP 48	00/06	01/06	00/06	00/06	00/06	00/06	00/06	00/06
PLCC 84	03/06	04/06	04/06	03/06	00/06	03/06	04/06	06/06

The intent of the design of the experimental runs listed in Table 9 was to compare the several combinations of solder paste, substrate finish, and T_g; two designed experimental matrices were chosen using a full factorial for the baseline tin-lead and SAC305, and a Latin Square for the low melt products (Table 11).

The Latin square design of order three is shown below in Table 10 and Table 11 . In general, the rows represent levels of one factor, the columns, another factor, and numbers in the cells, levels of a third factor. The Latin Square is a subset of all possible combinations, where each level of one factor is present with each level of another factor. The advantage is that the Latin Square provides estimates of factor level differences in a fraction of the possible combinations. In this case, the Latin Square of order 3 uses 9 combinations rather than the 27 required for a full factorial experiment [14].

Table 10: General Latin Square

	a	**B**	**c**
A	**1**	**2**	**3**
B	**3**	**1**	**2**
C	**2**	**3**	**1**

The T_g factor only has two levels of interest, so the high level was duplicated as the middle level. This is a common practice when one factor has fewer levels than the other two and presents only a minor complication in the analysis. Essentially, the difference between the high and middle levels is known to be equal to zero.

Table 11: Latin Square of Paste and Finish

		Finish		
		OSP	**ENIG**	**ENEPIG**
PASTE	**Paul**	**155**	**170**	**170**
	Violet	**170**	**155**	**170**
	Orchid	**170**	**170**	**155**

The factorial portion uses factors relevant to the traditional tin-lead pastes. In this case, each factor only had two levels of interest, so the traditional 2x2x2 layout was used.

The run data was summarized as pass/fail for each component and is shown in Table 9. Most of the BGAs and QFPs failed within the first two hours of 5G dwell. Components PLCC84 had some failures during the 5G dwell, and components SSOP48 had fewer failures.

The initial analysis intent was to use the time to failure as a variable Y (either an estimate of MTBF or time to first failure in the group). This would have been an ANOVA to look for any main effects that work consistently across the levels of the other factors. Because we only ran for only approximately one million cycles, several parts did not fail, limiting the variable analysis. The use of the fraction failing in each group was a possibility but didn't give us much to work with since the number of samples was small.

The analysis is mainly an inspection of the cube plots with the 3rd factor as the point color using Minitab 16. Since we are really looking for a potential combination of paste and finish that works across components (and, to a certain extent, T_g), the data is not so much an analytical conclusion with statistical calculations but, rather, an elimination of the obvious (*i.e.*, the near impossible possibilities) to find the area for the next experiment. Essentially, this experiment was a screening experiment. To this end, in Figure 39 the results of the full factorial show the combination OSP, SnPb, and T_g = 155°C to be the most robust for the component types PLCC84, 352BGA, 240QFP, and SSOP48. Although, for the SSOP48, all combinations worked well except OSP / SAC305 / T_g =170°C. In Figure 39, the results of the Latin squares shown in circles in the figure that the combination OSP / Violet / T_g =170°C to be the most robust for the component types PLCC84, 352BGA, 240QFP, and SSOP48.

Failure data also exists for the 2G harmonic vibration. Table 12 lists the results for 48 components each for Paul, Violet, and Orchid solders, with no failures in BGAs and SSOPs. Considering all of the components, Violet had two combinations where all the components survived, Paul had one combination where all components survived, and Orchid had none. In Figure 41, observe that when the 5G and 2G harmonic are juxtaposed, the survival trend stays intact, namely, Violet survives the longest, then Paul, then Orchid. This is the same trend that was observed in 5G testing. Furthermore, the Paul and Violet pastes in the 5G environment act more like the SnPb solder paste and less like the SAC305, which is showing higher failures.

Details

Table 12: Resistance Monitoring Failure Details for 2G Test

Card #	R239006	R239003	R239010	R246001	R246008	R246011	R247004	R247008	R247011
Paste type	Paul			Violet			Orchid		
Finish	OSP	ENIG	ENEPIG	OSP	ENIG	ENEPIG	OSP	ENIG	ENEPIG
T_g	155	170	170	170	155	170	170	170	155
352 BGA	00/02	00/02	00/02	00/02	00/02	00/02	00/02	00/02	00/02
240 QFP	02/02	00/02	00/02	00/02	02/02	00/02	02/02	02/02	01/02
SSOP 48	00/06	00/06	00/06	00/06	00/06	00/06	00/06	00/06	00/06
PLCC 84	01/06	00/06	02/06	00/06	00/06	00/06	00/06	04/06	00/06

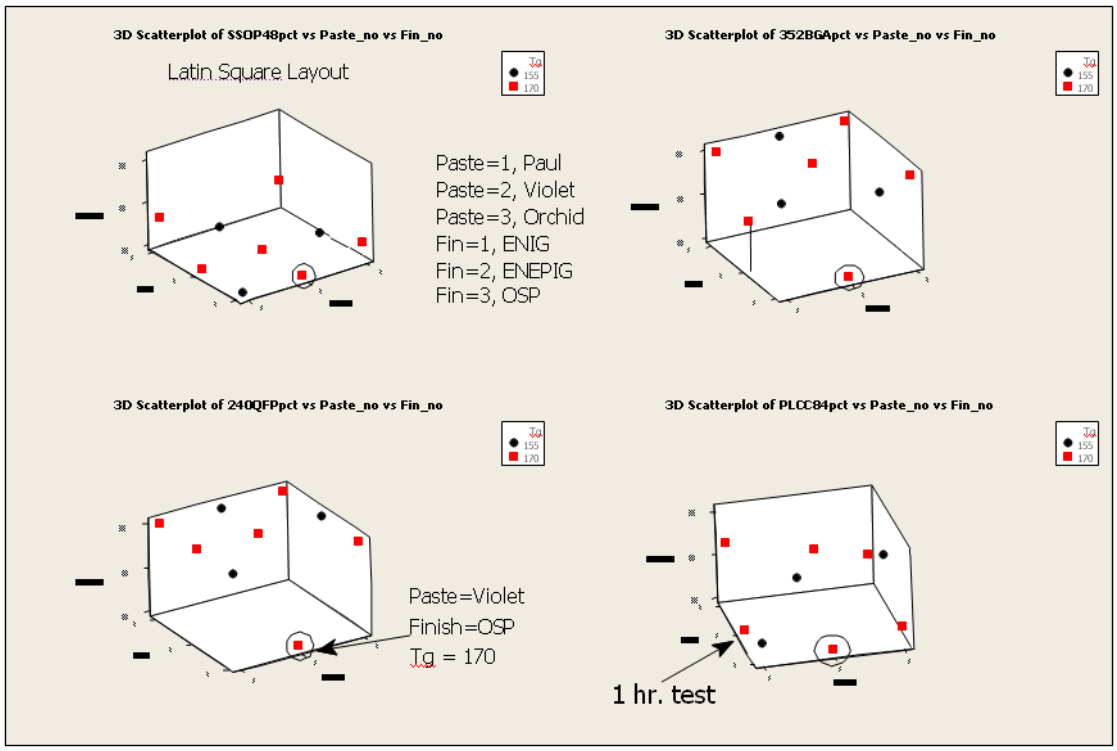

Figure 39: The 3D scatter plots for SnPb & SAC305 solder paste, finish, and T_g versus percentage failed at 5G harmonic dwell at first resonance frequency [15]

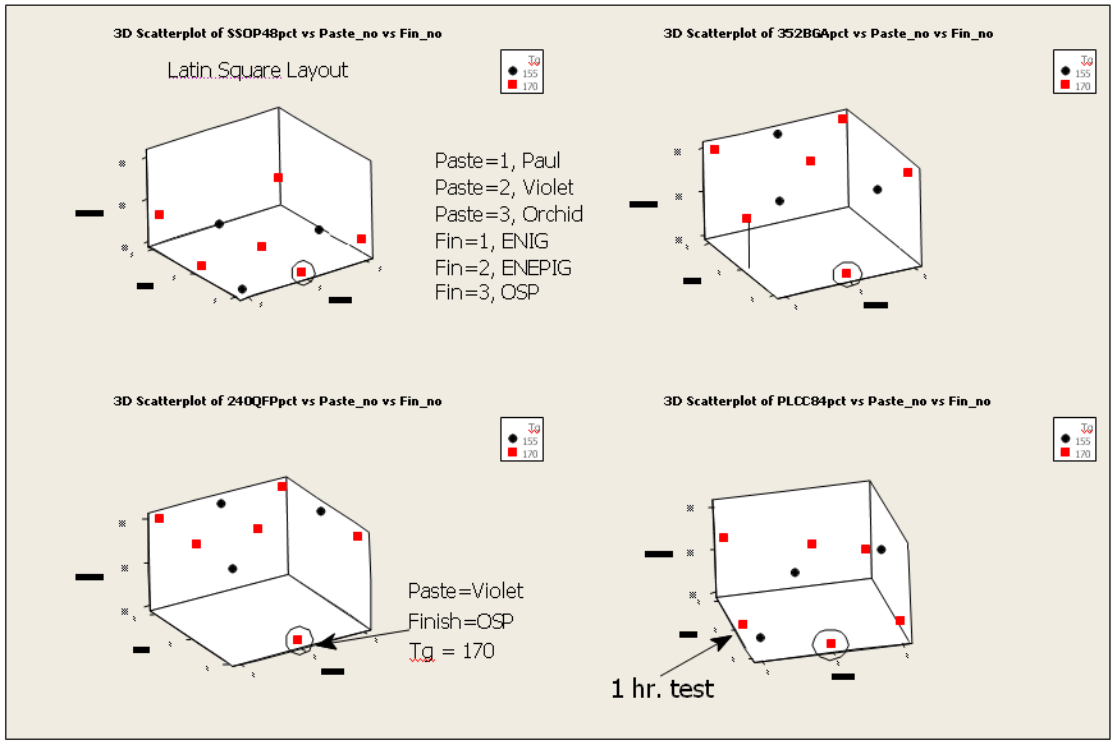

Figure 40: The 3D scatter plots for solder paste, finish, and T_g versus percentage failed at 5G harmonic dwell at first resonance frequency [15]

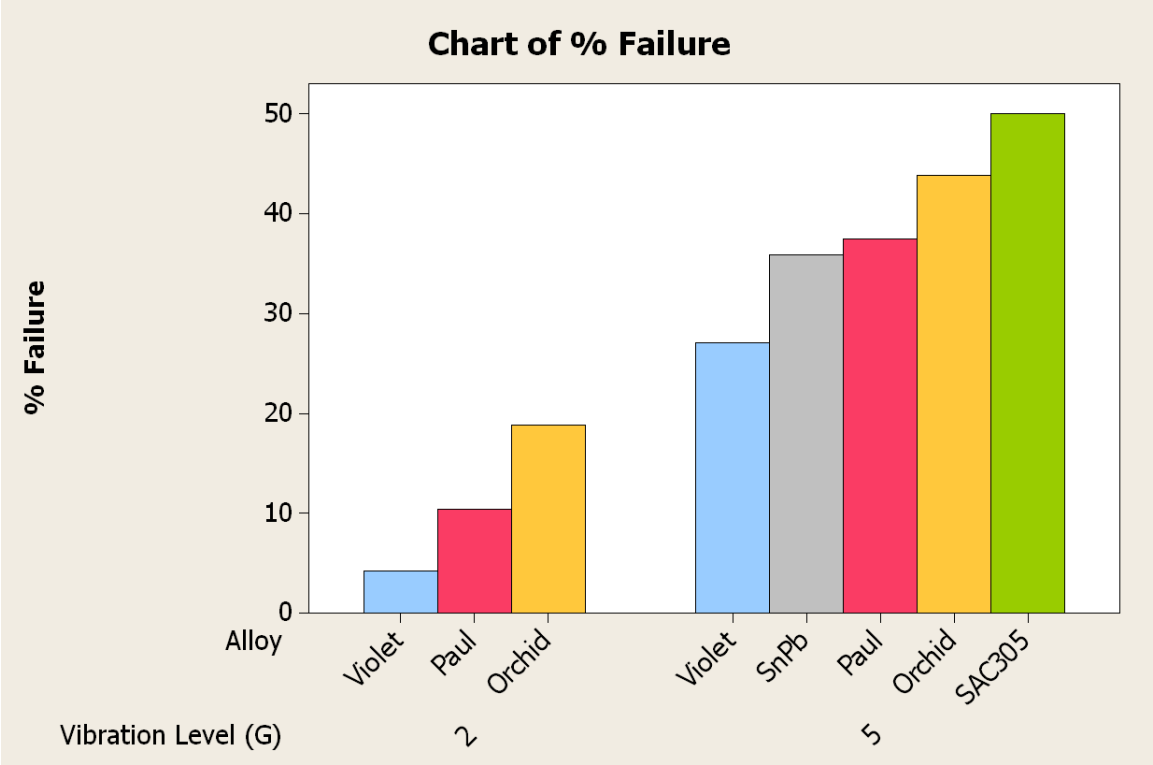

Figure 41: Percent Failed Components - 352 BGA, 240 QFP, SSOP 48 and PLCC 84 - After 6 Hours of Dwell at 2G and 5G Vibration

Metallurgical analysis

Failure analysis focused on four component types: 352 BGA, 240 QFP, SSOP 48 and PLCC 84.

There was no BGA failure after 2G vibration. 20% of BGAs assembled on 155°C T_g boards and 82.2% of BGAs assembled on 170°C T_g boards failed after 5G vibration. Typically, the BGAs failed through the solder either at the component side as illustrated in Figure 42, or closer to the board side in which case the copper pad was also damaged as illustrated in Figure 43.

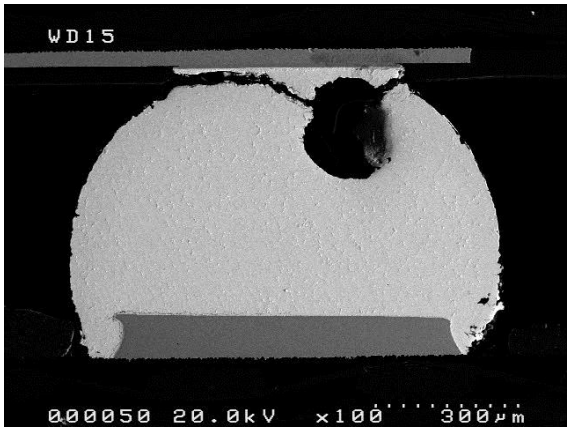

Figure 42: BGA with SAC305 on ENEPIG finish, 170 T_g board

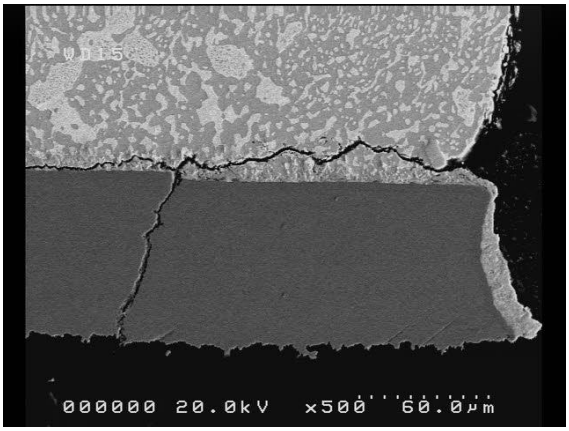

Figure 43: BGA with SnPb on ENEPIG finish, 170 T_g board

Board material had noticeable impact on the failure modes; 170°C T_g and in some cases 155°C board materials experienced failure via pad cratering as seen in Figure 44. This failure occurs at locations where the copper pad has cracked through. 155°C T_g boards where observed to have failures in the vias in the form of barrel cracks.

Surface finish also had an impact on the failure mode: All BGA failures on boards with OSP finish occurred through the solder as illustrated in Figure 45. ENEPIG failures occurred mainly in the same fashion, through the solder as shown in Figure 46 and Figure 47 with the exception of those failures which occurred with Orchid solder paste on ENEPIG finished boards. As shown in Figure 48, these failed through the brittle IMC layer formed between the solder and the board side copper pad with ENEPIG finish. All ENIG failures resulted from separation of the IMC from the board as shown in Figure 49.

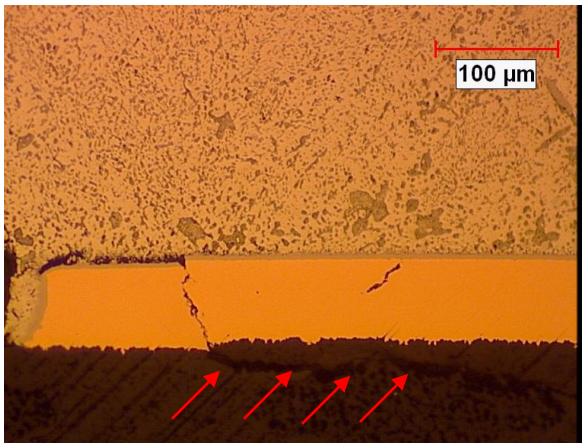

Figure 44: Board Side Failure (with Pad Crater) of BGA with SnPb Solder on ENEPIG Finish, 170 T_g Board

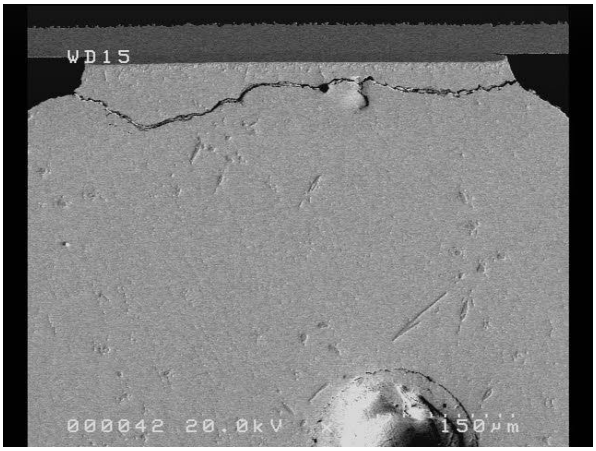

Figure 45: Component Side Failure with SAC305 Solder on OSP Finish, 170 T_g Board

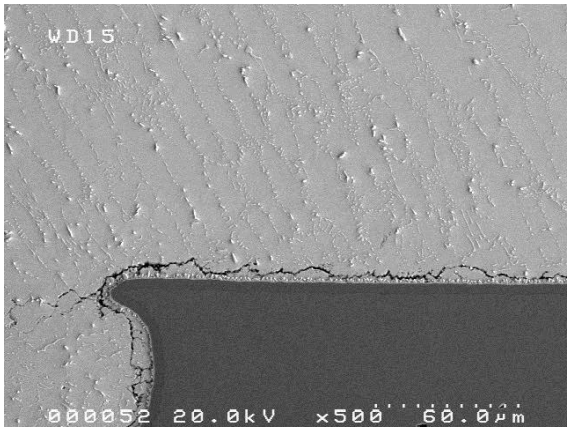

Figure 46: Board Side Failure of BGA with SAC305 Solder on ENEPIG Finish, 170 T_g Board

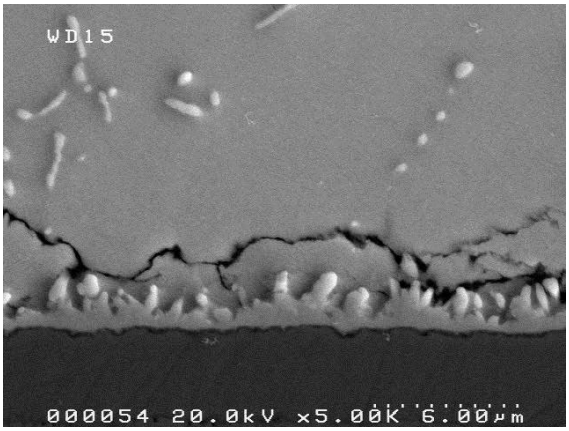

Figure 47: Board Side Failure of BGA with SAC305 Solder on ENEPIG Finish, 170 T_g Board

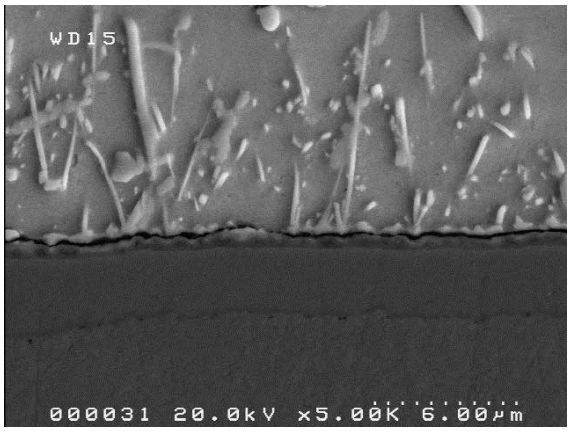

Figure 48: Board Side Failure of BGA with Orchid Solder on ENEPIG Finish, 170 T_g Board

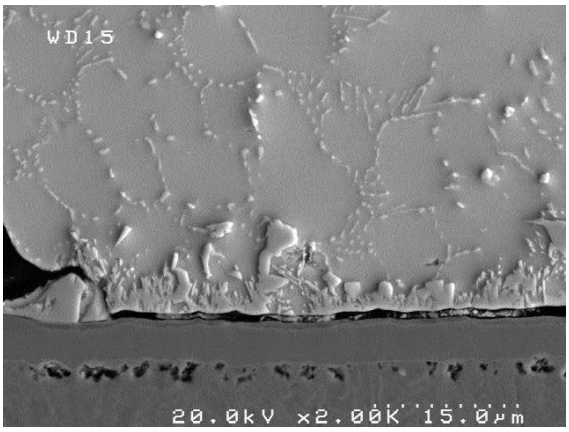

Figure 49: Board Side Failure of BGA with Paul Solder on ENIG Finish, 170T_g Board

No failures occurred with Violet solder paste on OSP board finish. This solder-finish combination performed as well as SnPb on OSP and outperformed all other variations. Cross sections of this sample reveal good microstructural properties with a consistent, unbroken IMC layer as seen in Figure 50 and Figure 51.

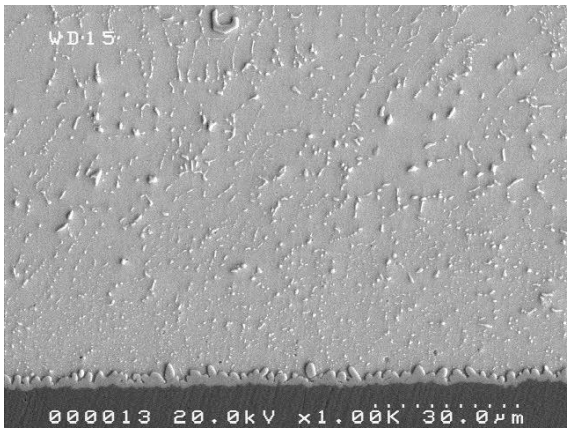

Figure 50: BGA with Violet Solder Paste on OSP Finish

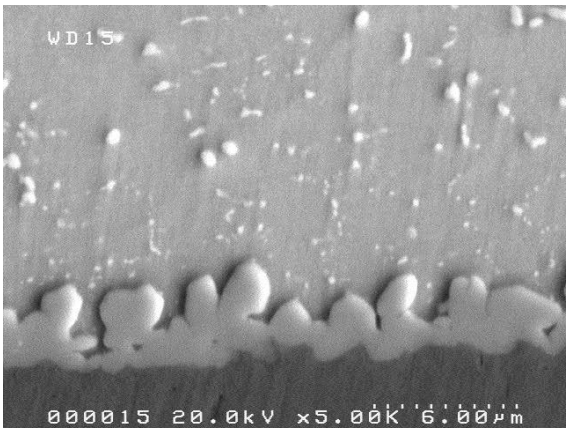

Figure 51: BGA with Violet Solder Paste on OSP Finish

QFP failures can be attributed to full cracks and breaks of the lead as revealed in Figure 52. The solder however does appear to be a factor as the crack initiation appears to occur within the solder along the lead as shown in Figure 53. Only Violet and SnPb solders appeared to have survived. No pad crater mode was detected in QFP solder joints nether in 170°C nor 155°C T_g boards. There was no difference in survival rate of QFPs assembled on 170°C and 155°C T_g boards as well. The pad crater failure mode is very typical for BGAs. There was a significant difference in survival rate between the BGAs assembled on 170°C and 155°C T_g boards. 80% BGAs assembled on 155°C T_g boards using Paul, Violet, Orchid and SnPb (SAC305 was excluded because 155°C T_g boards cannot be used for 240°C assembly) survived 1,000,000 cycles at 5G. Only 18.8% of the BGAs assembled using the same solder pastes on 170°C T_g boards survived 1,000,000 cycles at 5G. This suggests that the 155°C T_g laminate demonstrates a trend to pad crater failure mode reduction.

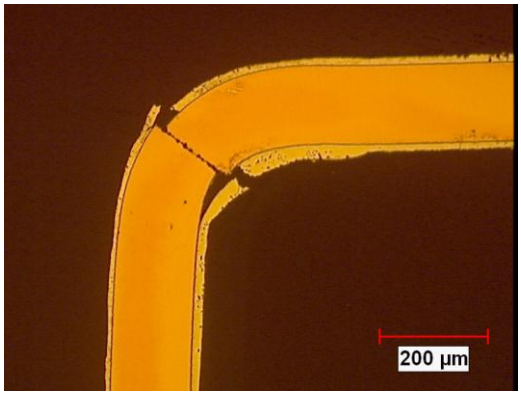

Figure 52: QFP Failure by Broken Lead

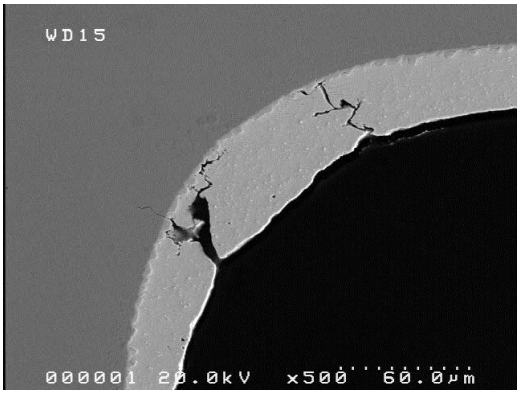

Figure 53: QFP Failure Initiating in Solder

Summary and Conclusions

The following results and conclusions may be made based on the results of the screening experiments on the manufacturability and reliability of lower melting Pb-free alloys which may satisfy aerospace requirements.

Three Bi-containing alloys: Sn3.4Ag4.8Bi (Paul) and two reduced Ag content variations, with and without Cu, Sn2.25Ag0.5Cu6Bi (Violet) and Sn2Ag7Bi (Orchid), were selected. Honeywell test vehicles were assembled using these alloys with processing temperatures about 10°C below that for SAC305. Two board materials with high T_g (170°C) and normal T_g (155°C) were used. The boards were finished with OSP, ENIG, and ENEPIG. No problems related to the manufacturability were detected. Experimental alloys had better wetting and less voiding than SAC305. The joints were properly formed, and were comparable to both SnPb and SAC305 joints.

The microstructural analysis after assembly revealed that

- All three Bi-containing alloys formed excellent joints on OSP finish. The interfacial intermetallic layer is comparable to SnPb in thickness and shape, and thinner than in SAC305.
- Sn3.4Ag4.8Bi (Paul) and Sn2Ag7Bi (Orchid) are not fully compatible with ENIG and ENEPIG, forming irregular and/or thicker interfacial intermetallic than SAC305. This is attributed to the lack of Cu in these alloy compositions.
- The alloy with Cu, Sn2.25Ag0.5Cu6Bi (Violet), is compatible not only with OSP, but also with ENIG and ENEPIG, and forms excellent solder joints with uniform intermetallic layers on both ball grid array and leaded components.
- On the ENEPIG finish, Pd-containing needle-shaped intermetallic particles are present in solder joints. These particles may cause solder joint embrittlement. The ENEPIG finish must be fully qualified for aerospace industry acceptance.

All combinations of alloys (Paul, Violet, Orchid, SAC305 and SnPb), surface finishes (OSP, ENIG and ENEPIG) and board laminate (normal and high T_g) passed the aerospace ATC qualification requirement of 1000 cycles of -55°C to 125°C. There was no solder joint failure on both high and normal T_g boards up to 3010 cycles for Pb-free lower melt and SAC305 alloys. However, there were via failures in normal T_g boards with OSP finish, assembled using all Pb-free and SnPb solders. Of these via failures on normal T_g OSP-finished boards, only the SAC305 cell did not meet the aerospace qualification requirement of 1000 cycles. All three experimental alloys Paul, Violet, and Orchid showed excellent performance in harsh environment thermal cycling.

An exceptional influence of bismuth additions on microstructural changes during thermal cycling was observed. Bi particles evenly precipitate in the tin matrix and reduce microstructure degradation.

The vibration failure results are based on one million cycles and show failure modes that might give an indication of what material combinations fail early. These observations for high reliability products are important benchmarks. Both 2G and 5G vibration levels showed a similar failure progression of the number of failures based on resistance measurements. The order of the failure stays the same. The lowest failure rate found was for Violet followed by Paul and Orchid at the 2 G level. Violet and Paul showed the lowest rate of failure at the 5G level, followed by SnPb and Orchid. The SAC305 had the highest failure rate. Our recommendation for future work would be to start at 5G and then to select the higher G level that would precipitate more representative failure modes for the given amount of test time. Paul and Violet responded more like SnPb than SAC305, and thus appear to be a consistent, lower melt, robust substitute for SnPb.

The failure mode of QFPs in vibration testing was full cracking of the copper leads, which were observed to have initiated in the solder that wicked up along the lead during reflow. BGAs failed in vibration most frequently due to cracking through the bulk solder and laminate material creating some degree of pad cratering. The cracks from the laminate material may propagate through the copper pad to the solder material, resulting in open joints. The 155°C T_g laminate material demonstrated a trend to pad cratering reduction compare to the 170°C T_g material. Both ENIG and ENEPIG finishes showed failures at the IMC; ENEPIG exhibited failure through the brittle IMC formed with Orchid solder pastes, whereas ENIG resulted in failure between the IMC and copper pad with all alloys.

These screening experiments provide some insight into the main effects of the alloy performance and show positive evidence for future study. Based on the results of the screening experiments, the lower melting alloys containing bismuth, particularly Violet and Paul, are recommended for further statistically valid reliability testing. The recommended testing will enable the choice of an alternative RoHS Pb-free alloy with lower process temperature and better thermomechanical properties.

Future work

There is still much exploration yet to do before the new lower melt bismuth-containing alloys are ready for RoHS compliant product introductions. Currently, the developments are at a NASA technology readiness level (TRL) 3. The goal over the next few years is to raise the readiness to TRL 7. The next work will be in cooperation with a NASA Phase 3 project proposal to leverage these results into a larger matrix with additional exposures and larger sample sizes for a continued reliability study. The draft plan for this work is in progress with multiple aerospace company representatives. Subject matter experts will be leveraged within this effort and will help advance the study of the alloy reliability within their sectors. In addition, Celestica is in pursuit of technical partners to continue other reliability studies. Proposals have been made with other aerospace sector companies to leverage government funding for the expansion of the knowledge on these interesting alloys. The goal is to have enough data to permit the use of the alloy in a product trial and field test to validate the performance, which could launch a potential product-level solution for aerospace products that can comply with the environmental initiatives of the larger electronics products community.

Acknowledgements

The authors would like to thank the following individuals from Celestica: Russell Brush, Alon Walk, Kangwon Lee, Veseyathaas Thambipillai for ATC testing and data analysis; Jie Qian for sample preparation; Jose Traya and Michael Emery for test vehicle assembly; Suthakaran Subramaniam and Michelle Le for vibration testing; and Dr. John Vic Grice, Honeywell Corporate consulting statistician who helped design the experimental matrix. The authors would also like to acknowledge Holaday Circuits for providing the different laminate board materials used in the evaluations.

References

[1] http://www.teerm.nasa.gov/nasa_dodleadfreeelectronics_proj2.htm.
[2] “Properties of Ternary Sn-Ag-Bi Solder Alloys: Part 1- Thermal Properties And Microstructure Analysis”, P. Vianco, et al. Journal of Electronic Materials, Vol.28, pp. 1127-1137, 1999
[3] “Properties of Ternary Sn-Ag-Bi Solder Alloys: Part 2- Wettability and Mechanical Properties Analysis”, P. Vianco, et al. Journal of Electronic Materials, Vol.28, No.10, pp. 1138-1143, 1999.
[4] “Creep Behavior of Bi-Containing Lead-Free Solder Alloys”, D. Witkin, et al. Journal of Electronic Materials, Vol. 41, No.2, pp. 190-203, 2012.
[5] “Lead-Free Electronics: iNEMI Projects Lead to Successful Manufacturing”, E. Bradley, C. A. Handwerker, J. Bath, R. D. Parker, R. W. Gedney , 472 pages, 2007.
[6] http://www.freesamplesite.com/ydf/showthread.php/149076-Free-NCMS-Lead-Free-Solder-Project-CD-Rom

NSMS, Lead-Free, High-Temperature, Fatigue-Resistant Solder: Final Report, Ann Arbor, MI: National Center for Manufacturing Science, 2001.
[7] http://www.aciusa.org/leadfree/LFS.../02_GREENE_JG-PP_JCAA_Program.pdf.
[8] "Conception and Production of high reliable PWB-assemblies for thermally and mechanically highly stressed long term reliable lead free electronic systems for Aeronautics" Dr. Ing. G. Reichelt, German Joint Project. PERM # 8, Noordwijk, 2011.
[9] "New Generation Of Lead-Free Solder Alloys: Possible Solution To Solve Current Issues With Main Stream Lead-Free Soldering", P. Snugovsky, S. Bagheri, M. Romansky, D. Perovic, L. Snugovsky, J. Rutter, SMTA Journal, Vol. 25 Issue 3, 2012.
[10] "Assembly Feasibility and Property Evaluation of New Low Melt Solder Alloys", E. Kosiba, et al., ICSR SMTA Proceedings, Toronto, 2012.
[11] "Manufacturability and Reliability Screening of Lower Melting Point Pb-Free Alloys Containing Bi", P. Snugovsky et al., IPC APEX EXPO Conference Proceedings, San Diego, 2013.
[12] Woodrow, T.A., "NASA-DoD Lead-Free Electronics Project: Vibration Test", Boeing Electronics Materials and Processes Report - 603, June 30, 2010
[13] NASA-DoD Lead-Free Electronics Project Plan, August 2009.
[14] "Design and Analysis of Experiments", Montgomery, D.C., 7th edition. John Wiley & Sons, 2009.
[15] Minitab 16 Statistical Software, www.minitab.com

APEX EXPO IPC
NEW IDEAS ... FOR NEW HORIZONS
MARCH 25-27, 2014
MANDALAY BAY RESORT AND CONVENTION CENTER
LAS VEGAS, NEVADA

Reliability Screening of Lower Melting Point Pb-Free Alloys Containing Bi

Honeywell
Arizona, USA

Joseph M. Juarez, Jr.,
Michael Robinson,
Joel Heebink

joseph.juarez@honeywell.com
mike.robinson6@honeywell.com

Celestica, Inc.
Toronto, Canada

Polina Snugovsky,
Eva Kosiba,
Jeffrey Kennedy,
Zohreh Bagheri,
Subramaniam Suthakaran,
Marianne Romansky,

polina@celestica.com

Problem Statement .

- Aerospace and defense organizations exercise RoHS exemptions and research reliability for RoHS compliant solders
- Aerospace and Military products need better
  - vibration performance
  - drop/shock performance
  - combined environment reliability

  than RoHS SAC305 alloy
- Pad cratering is a dominant failure mode especially under dynamic loading

http://www.navy.mil/navydata/aircraft/fa18/shornet2.html

Flight deck avionics controls and displays [1]

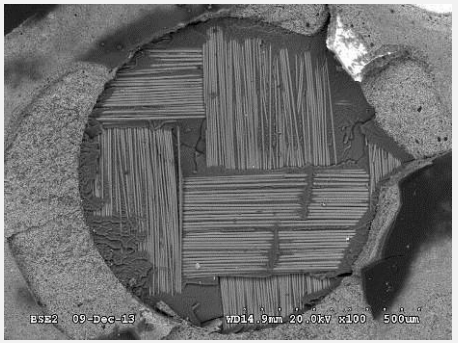

Image prepared by Zohreh Bagheri, Celestica

[1] Photo Credit: Boeing Photo Neg. #K58380 downloaded from Boeing Home/Images/Image Gallery/Commercial Airplanes/In Production/777

Possible Solution

- Pb-free solders with lower process temperatures
  - Reduces thermal damage to boards and components
  - Lower Tg board materials are less prone to pad cratering defects

- Several Sn-Ag-Bi and Sn-Ag-Cu-Bi alloys are available
  - Melt about 10° C lower than SAC305.
  - Bismuth
    - Reduces melting temperature
    - Improves thermomechanical behavior
    - Reduces propensity to whisker growth
    - Not used due to Sn-Pb-Bi low melting ternary eutectic (96° C) and peritectic (137° C)

Time to use Bi containing alloys.

Pb has been removed from component finishes

Background

- Celestica Pb-free lower melt alloy program began in 2009
- Objective:
  - Select new Pb-free solder alloys with process temperatures comparable to conventional SnPb solder for assembly and rework of all component types

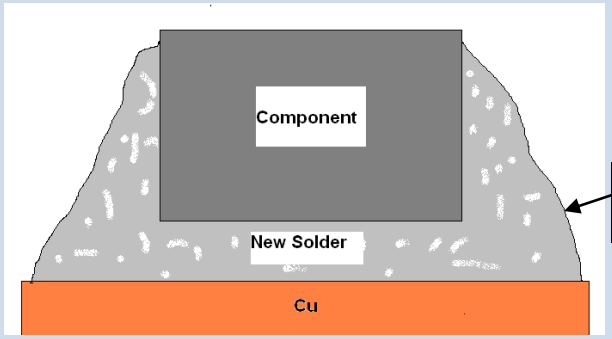

1. Leaded and discrete components

New solder

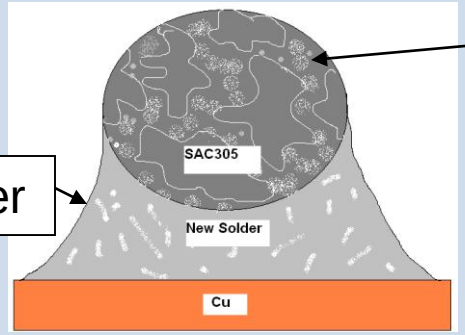

2. Ball grid alloy components

  - Use of standard laminate materials
  - Low Ag or no Ag alloys cheaper and more compliant
  - Interconnects with improved mechanical and thermal mechanical performance

Background

- The conversion to RoHS-compliant Pb-free assembly has been a considerable challenge to the electronics assembly industry
  - One of the main reasons is the **higher reflow process temperatures** required for Pb-free assembly
  - These higher temperatures can **thermally damage the PCB and components**
  - High Tg board materials used with the main stream Pb-free solder SAC305 are prone to **Pad Cratering**
    - Pad Cratering is a latent defect that occurs during assembly/rework and post assembly handling and testing. It cannot be identified during back end of line in-circuit (ICT) or functional test (FCT) protocols and poses a high reliability risk under mechanical and thermo mechanical loading.

Pad Cratering is a main failure mode in field conditions

Benefits

1. Low melting temperature
   - Reduce process temperature
   - Use cheaper board material -normal T_g
   - Mitigate pad cratering
   - Reduce de-lamination and cracking caused by entrapped moisture
   - Reduce warpage
   - Reduce Pad-in-Pillow
   - Eliminate baking
   - Use temperature sensitive components
2. No or low Ag
   - Prevent Ag_3Sn platelets formation
   - Better mechanical properties - reduced toughness
   - Cheaper than SAC 305
   - More environmentally friendly

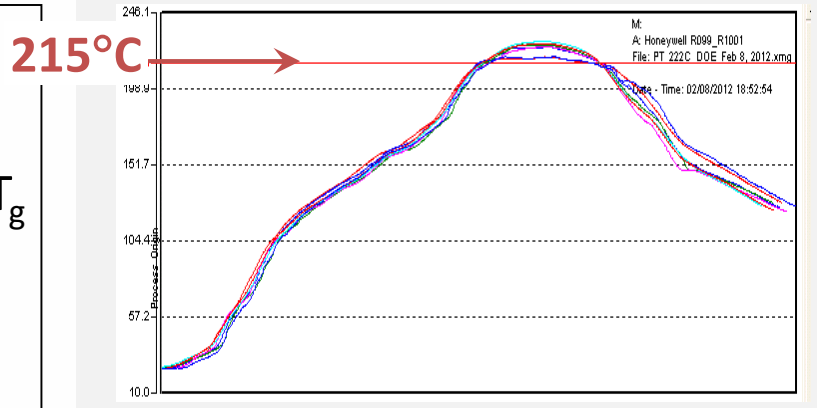

Typical reflow profile for normal T_g boards

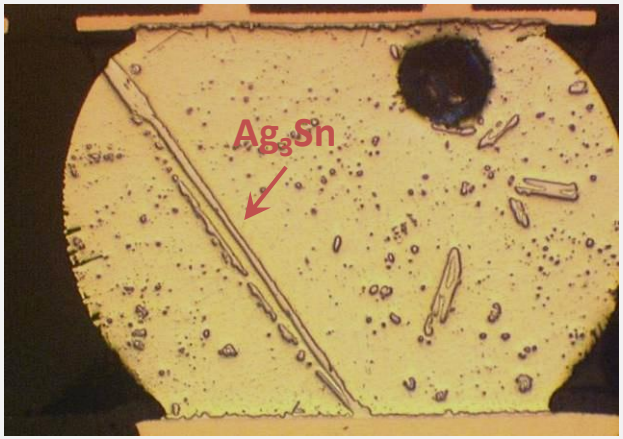

Image prepared by Zohreh Bagheri, Celestica

Benefits

3. Bi in composition
   - Better mechanical properties – better performance under vibration
   - *Reduce whisker propensity*

4. Cu and Bi in composition together with lower process temperature
   - Cu dissolution should not be such a problem

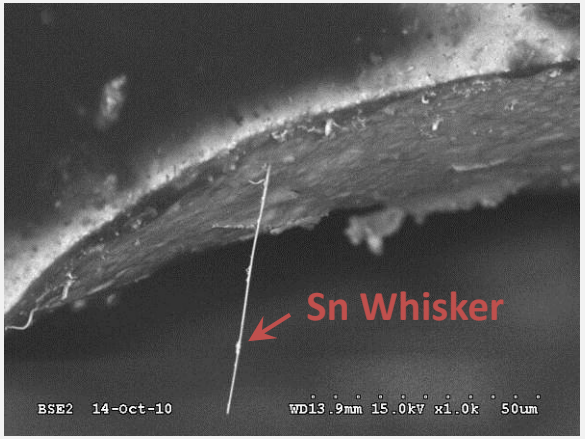

Image prepared by Zohreh Bagheri, Celestica

Results to Date

- Phase 1:
  - Alloys selection, Celestica & University of Toronto – 2009

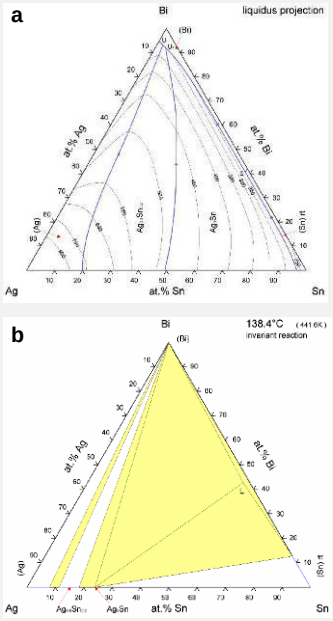

Ag-Bi-Sn Phase Diagrams showing:
a) liquidus projection and b)138.4°C

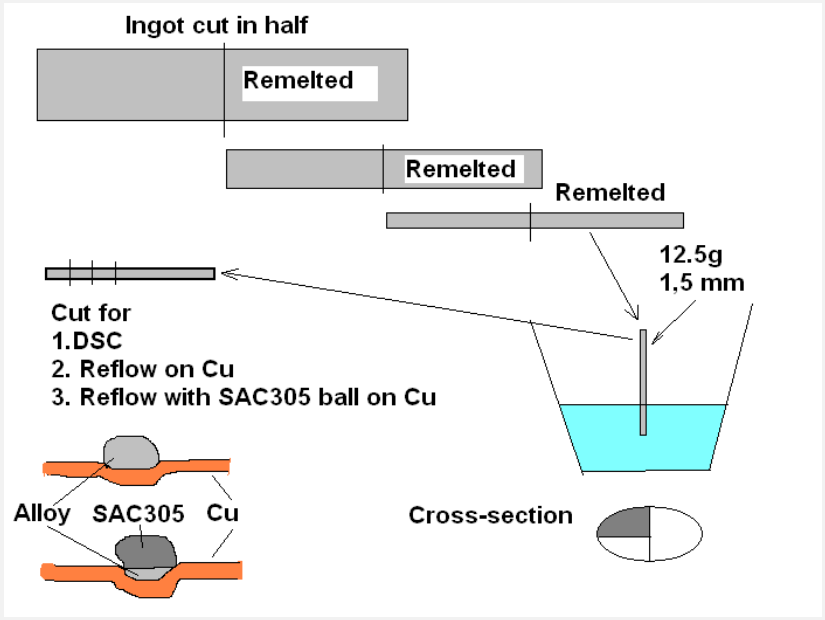

Illustration of initial alloy processing and analysis

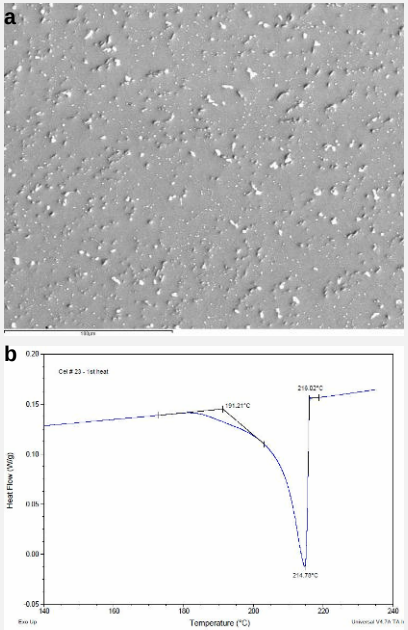

Alloy evaluation via a) cross sectioning for microstructural evaluation and b) DSC analysis of melting range

Results to Date

- Phase 2:
  - Manufacturing feasibility, Celestica – 2010
- Phase 3:
  - Screening experiments, Celestica &Customers – 2011-2013
    - Consumer electronics
    - Telecommunications
    - Aerospace
      - **APEX2013 Celestica/Honeywell**

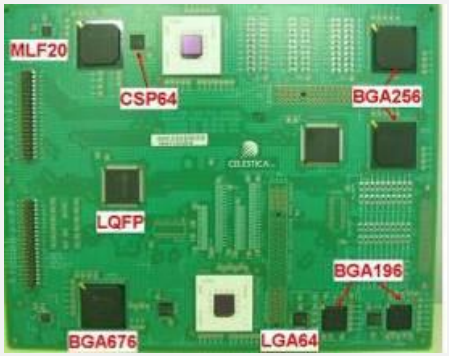

Celestica's RIA3 test vehicle used to evaluate manufacturing feasibility

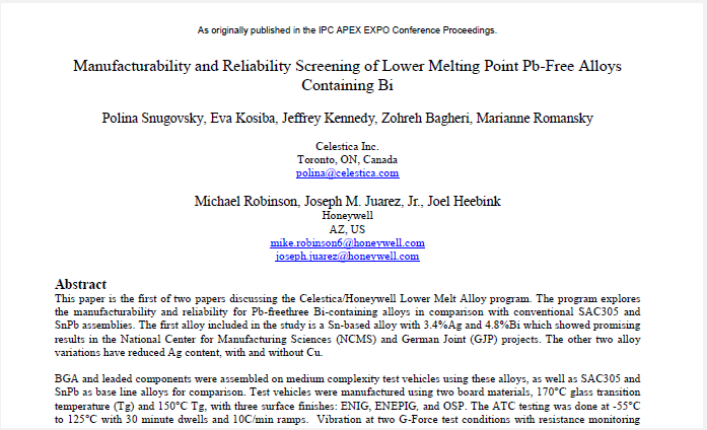

As originally published in the IPC APEX EXPO Conference Proceedings.

Manufacturability and Reliability Screening of Lower Melting Point Pb-Free Alloys Containing Bi

Polina Snugovsky, Eva Kosiba, Jeffrey Kennedy, Zohreh Bagheri, Marianne Romansky

Celestica Inc.
Toronto, ON, Canada
polina@celestica.com

Michael Robinson, Joseph M. Juarez, Jr., Joel Heebink
Honeywell
AZ, US
mike.robinson6@honeywell.com
joseph.juarez@honeywell.com

Abstract

This paper is the first of two papers discussing the Celestica/Honeywell Lower Melt Alloy program. The program explores the manufacturability and reliability for Pb-freethree Bi-containing alloys in comparison with conventional SAC305 and SnPb assemblies. The first alloy included in the study is a Sn-based alloy with 3.4%Ag and 4.8%Bi which showed promising results in the National Center for Manufacturing Sciences (NCMS) and German Joint (GJP) projects. The other two alloy variations have reduced Ag content, with and without Cu.

BGA and leaded components were assembled on medium complexity test vehicles using these alloys, as well as SAC305 and SnPb as base line alloys for comparison. Test vehicles were manufactured using two board materials, 170°C glass transition temperature (Tg) and 150°C Tg, with three surface finishes: ENIG, ENEPIG, and OSP. The ATC testing was done at -55°C to 125°C with 30 minute dwells and 10C/min ramps. Vibration at two G-Force test conditions with resistance monitoring

Alloy Selected for High Reliability Screening Experiments

Celestica Name	Alloy Constituents	Alloy Composition	Min Melting Temperatures, ° C (Experimental)	Melting Range, ° C
Paul	SnAgBi	Sn ***3.4%***Ag ***4.8%***Bi	206	11
Violet	SnAgCuBi	Sn ***2.25%***Ag ***0.5%***Cu ***6.0%***Bi	205	10
Orchid	SnAgBi	Sn ***2.0%***Ag ***7.0%***Bi	190	25
SAC305	SnAgCu	Sn ***3.0%***Ag ***0.5%***Cu	217	6
Eutectic SnPb	SnPb	Sn ***37.0%***Pb	183	0

Alloy Selection

- **Paul** **Sn 3.4%Ag 4.8%Bi** was proposed by Paul Vianco
  - Excellent pasty range
  - Excellent thermomechanical properties for harsh environments
    - proved by NCMS and the German Joint Lead-Free Avionics project
- **Violet** **Sn 2.25%Ag 0.5%Cu 6.0%Bi** is a variant of "Paul"
  - Excellent pasty range
  - Lower Ag content, does not form Ag_3Sn plates
    - may help to improve drop/shock properties
  - Cu to reduce the Cu dissolution potential
  - Higher Bi related to reduced Ag may help to better mitigate whisker formation
- **Orchid** **Sn 2.0%Ag 7.0%Bi** is a variant of the "Paul"
  - Pasty range is wider than in alloys #1 and #2
  - lower Ag and higher Bi
    - reduction of the minimum melting temperature.
  - may show greater whisker mitigation
- **SAC305** and Sn-Pb solders were included in the test matrix for comparison

Test Vehicle

- Honeywell designed
- Used for numerous Sn-Pb baseline and Pb-free process development
- Board stack-up and dimensions are representative of a large percentage of aerospace products
- Designed per IPC-4101/126 & /129 requirements

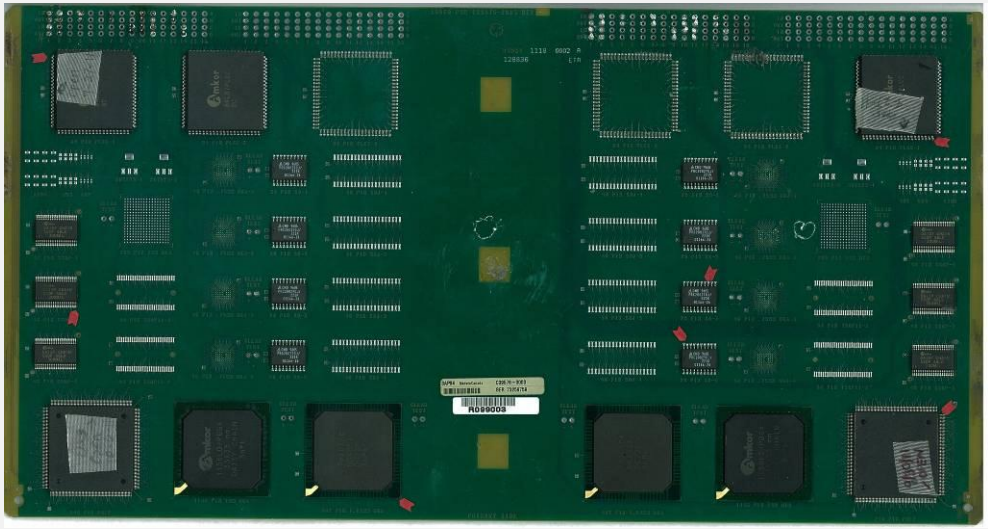

- 203mm x 355mm and 2.5mm
- 16 layers of alternating signal and ground/power plane with copper
- Daisy chained

Solder paste

- No-clean solder pastes of the experimental alloys were produced by one of the major solder paste suppliers
- Solder paste performance evaluation was done using a standard Celestica solder paste evaluation procedure

Laminate materials

T_g (° C)	LAMINATE	SUPPLIER
155	Nelco 4000-7	Holaday Circuits
170	Isola 370HR	Holaday Circuits

Surface finishes

SURFACE FINISH	THICKNESS (µm)
OSP	Entek 106A (Copper Triazole)
ENIG	MacDermid Ni 3.81µm - 0.13-0.20µm Au
ENEPIG	Uyemura Ni 3.81µm – 0.05µm Pd – 0.08µm Au

Component types

I/O COUNT/ PACKAGE	DIMENSIONS, mm	PITCH, mm	LEAD FINISH	BALL COMPOSITION
20 SO	6.35 X 12.70	1.27	SnPb and Sn	
40 SOJ	10.16 X 25.40	1.27	SnPb and Sn	
48 SOP	5.08 X 15.24	0.50	SnPb and Sn	
54 TSSOP	10.16 X 21.59	0.64	SnPb and Sn	
84 PLCC	29.21 X 29.21	1.27	SnPb and Sn	
240 PQFP	31.75 X 31.75	0.50	SnPb and Sn	
289 BGA	17.15 X 17.15	1.02		SnPb and SAC305
352 BGA	35.56 X 35.56	1.27		SnPb and SAC305
1156 BGA	34.93 X 34.93	1.02		SnPb and SAC305

Assembly

- 56 test vehicles built at Celestica
- 7 thermocouples placed on the board
- Reflowed in a 10-zone Electovert Omniflow oven
- Siemens Siplace X3 SMT placement machine
- Visual and Xray

Build Matrix

BOARD MATERIAL	ALLOY	SURFACE FINISH		
		ENEPIG	ENIG	OSP
155°C T_g	SnPb	2		3
	SAC305	2		2
	Paul			4
	Violet		4	
	Orchid	4		
170°C T_g	SnPb	2		3
	SAC305	2	1	3
	Paul	4	4	
	Violet	4		4
	Orchid		4	4

Reflow Profile for 222°C (SnPb, New Alloys)

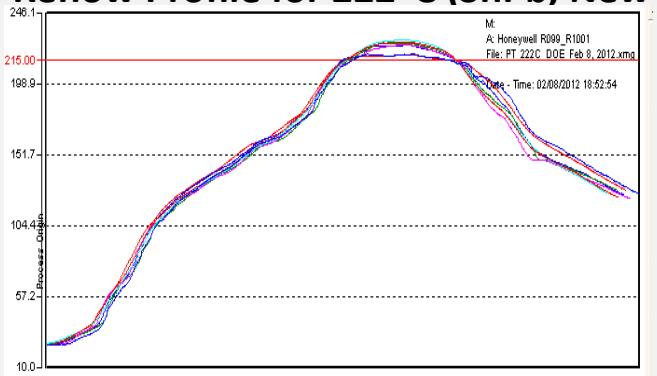

Reflow Profile for 240°C (SAC305)

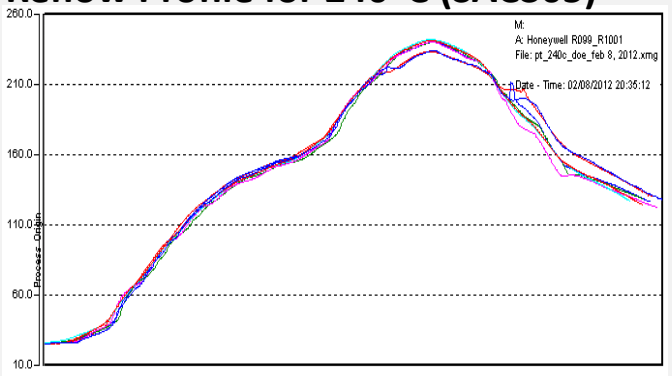

As Assembled Solder Joint Quality

- Acceptable solder joints in all assemblies
  - Voiding
  - Wetting
  - Shape and size
- No major anomalies or concerns
- Experimental alloys have less voiding than SAC305 and comparable to SnPb
- The lower level of voiding on ENEPIG followed by ENIG and then OSP
- Wetting on OSP is improved for the experimental alloys containing Bi
- Detailed microstructure analysis published in the APEX2013 paper

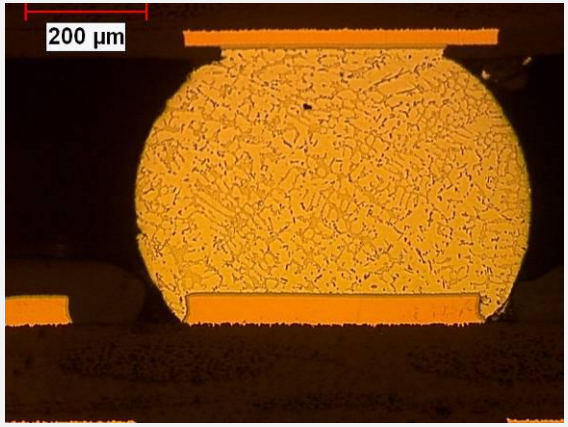

Cross Section of As Assembled BGA Solder Joint

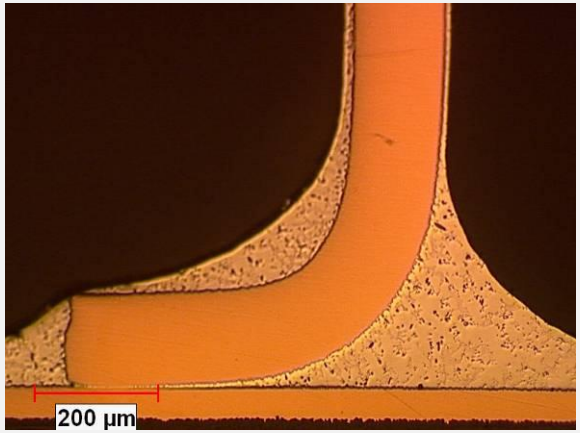

Cross Section of As Assembled QFP Solder Joint

Test Strategy for Harsh Environment

- The solder interconnections are different under thermal cycling and mechanical shock loadings
- ATC target
  - -55°C to 125°C
  - 10°C/min ramp rate
  - 30 minute dwell at both extremes
  - 3000 cycles
- Vibration testing plan
  - 5G level and
  - 2G level
  - Resistance, strain and vibration recorded

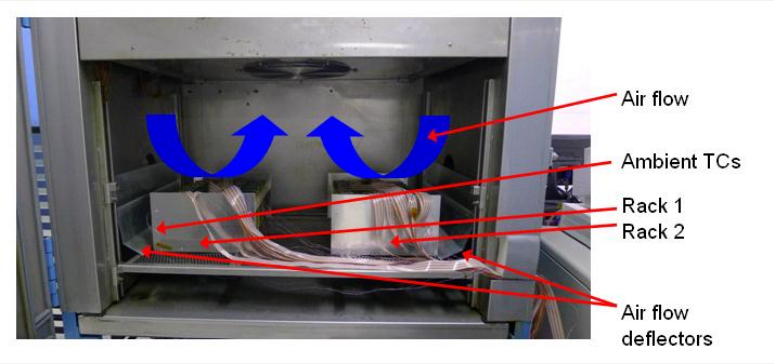

Boards loaded into ATC chamber, airflow direction indicated

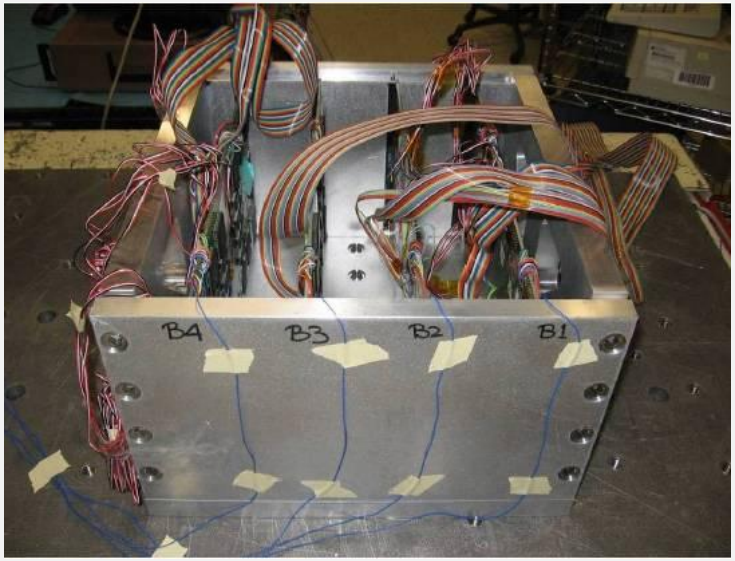

Fixture with Boards Mounted onto Vibration Table

ATC Testing

- Analysis Tech STD-256 event detectors
- A failure recorded when the resistance increased to 300 Ω or more for at least 200ns
- Checked at room temperature to determine the location of failure
- 17 boards tested, 32 components monitored on each boards
- Selected failed components were cut from the board for detailed analysis
- The remaining components were returned to the chamber for further testing

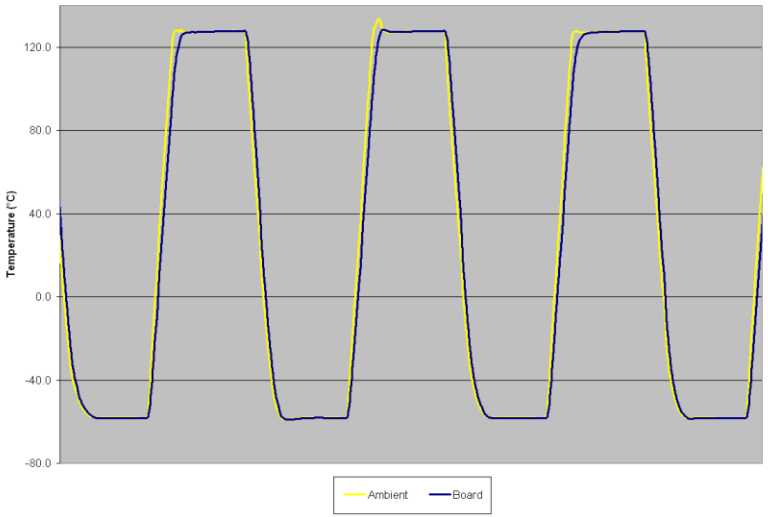

ATC Temperature Profile

Profile
- -58°C to 130°C
- 38 minutes in a hot dwell
- 39 minutes a cold dwell
- 13 minute ramp
- 103 minutes per cycle
- 3010 cycles completed

ATC Failure Analysis

- BGAs and QFPs were resistance monitored throughout ATC
- Periodically, the chamber was stopped and the recorded failures where verified by hand measurement at room temperature
- Components with confirmed failures were cut out of the board for failure analysis
  - Failures were cross sectioned to the failure location
  - Both the via and the solder joint were evaluated
- Boards were then returned to chamber and testing resumed
- No electrical fails recorded on QFPs, however QFPs cross sectioned in order to evaluate microstructural changes during ATC
- **155°C T_g boards were found to be failing in the vias (barrel cracks) as reported in APEX2013**

ATC Results and Analysis after 3010 cycles at -58° C to 130° C

- All alloy/finish/board combinations passed 1000 cycle industry requirements – except *SAC305/OSP/155 °C T_g*
- All electrical failures attributed to board failure (via cracks)
- Fatigue cracks found in failed BGAs
  - SnPb: near complete fatigue crack
  - Violet: partial fatigue crack

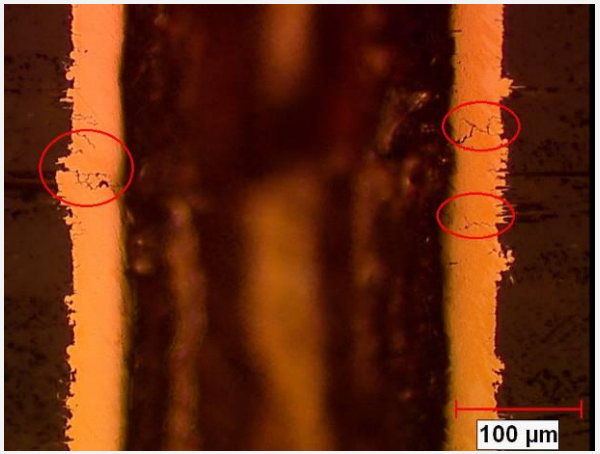

Cross Section showing barrel crack in via beneath SnPb/OSP/170°C T_g solder joint after 1734 cycles

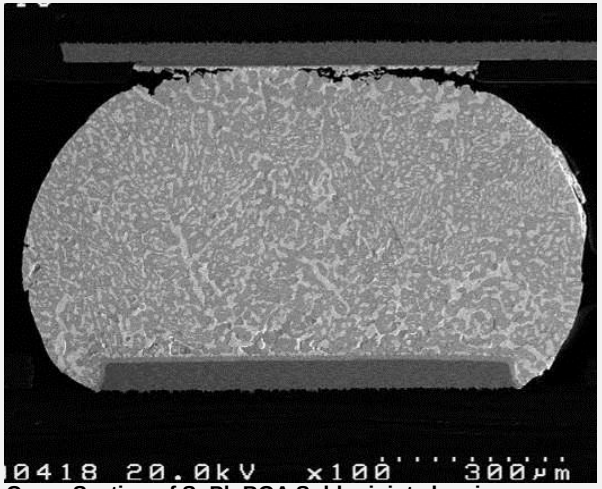

Cross Section of SnPb BGA Solder joint showing near complete fatigue cracking after 1734 cycles

ATC Results and Analysis after 3010 cycles at -58° C to 130° C

SnPb microstructural change after 3010 cycles ATC (seen on QFP)

- Recrystallization and Grain Growth
- IMC layer growth, Cu_3Sn phase now visible
- Pb (brittle phase) pooling at IMC layer

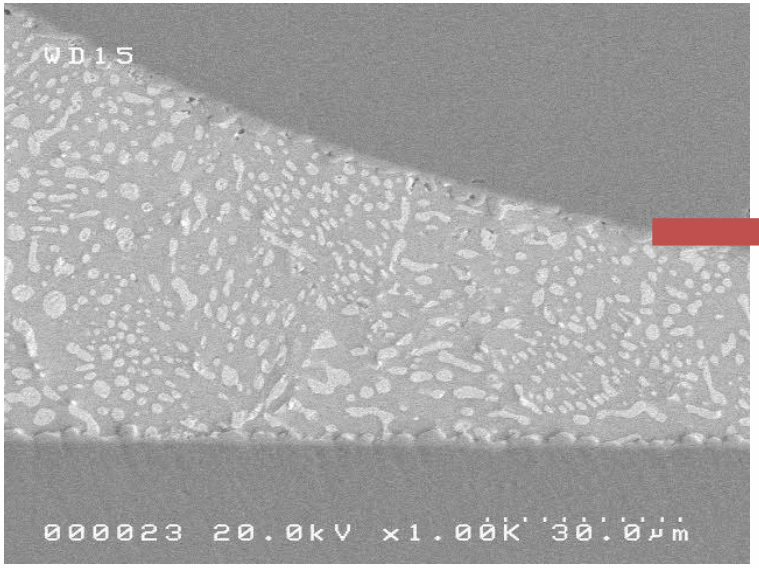

Cross Section showing SnPb microstructure after assembly

3010 cycles ATC

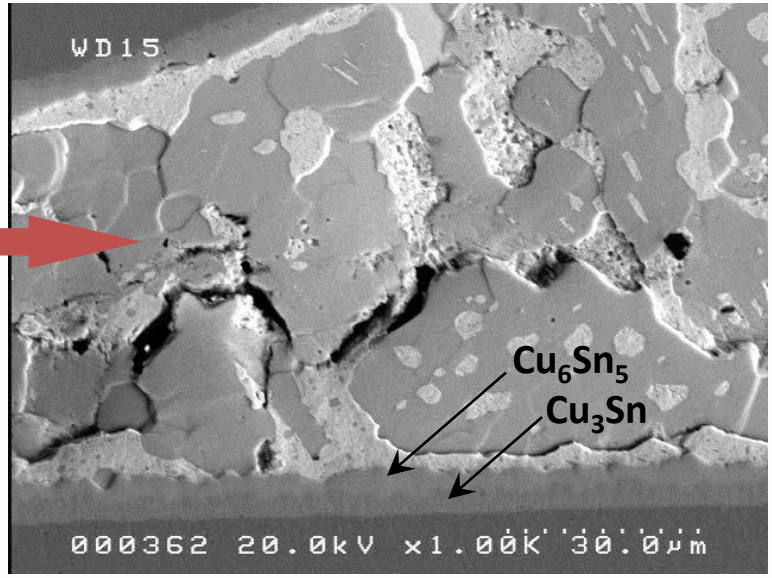

Cross Section showing SnPb microstructure after 3010 cycles of harsh environment ATC

ATC Results and Analysis after 3010 cycles at -58° C to 130° C

SAC305 microstructural change after 3010 cycles ATC (seen on QFP)

- grain growth, IMC layer growth
- Distinct Cu_3Sn layer in IMC after 3000 cycles
- Ag_3Sn particles coalesced into fewer, larger particles
- Incomplete crack propagating along the lead

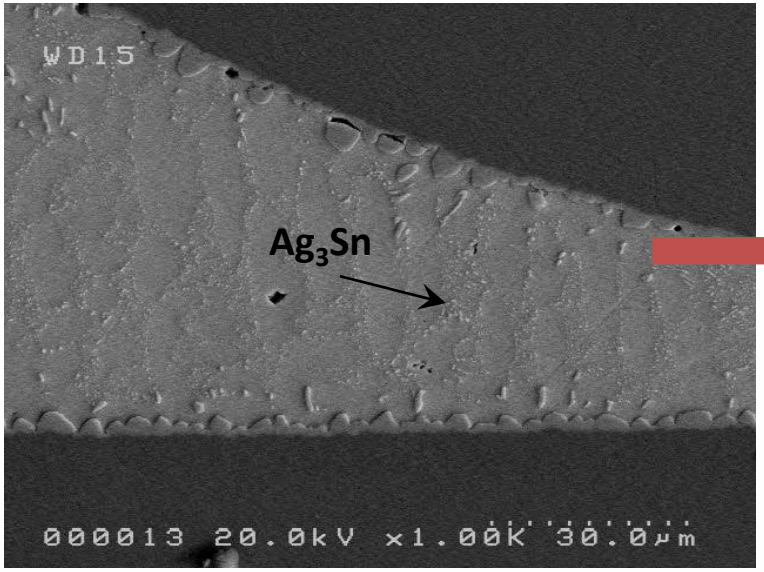

Cross Section showing SAC305 microstructure after assembly

3010 cycles ATC

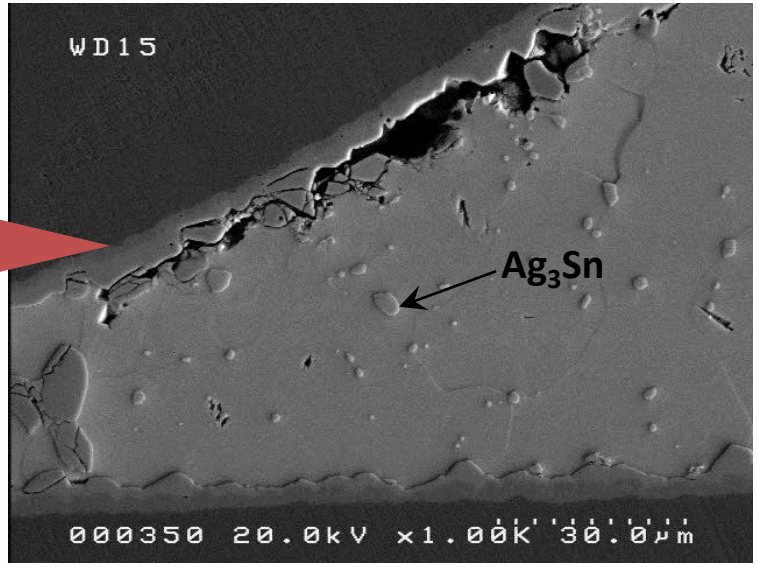

Cross Section showing SAC305 microstructure after 3010 cycles of harsh environment ATC

ATC Results and Analysis after 3010 cycles at -58° C to 130° C

Violet microsturtural change after 3010 cycles ATC (seen on QFP)

- IMC layer growth, Distinct Cu_3Sn layer in IMC
- Grains did not appear to grow
- Bi, present in solid solution in Sn at assembly, precipitated out of solution after 3010 cycles ATC

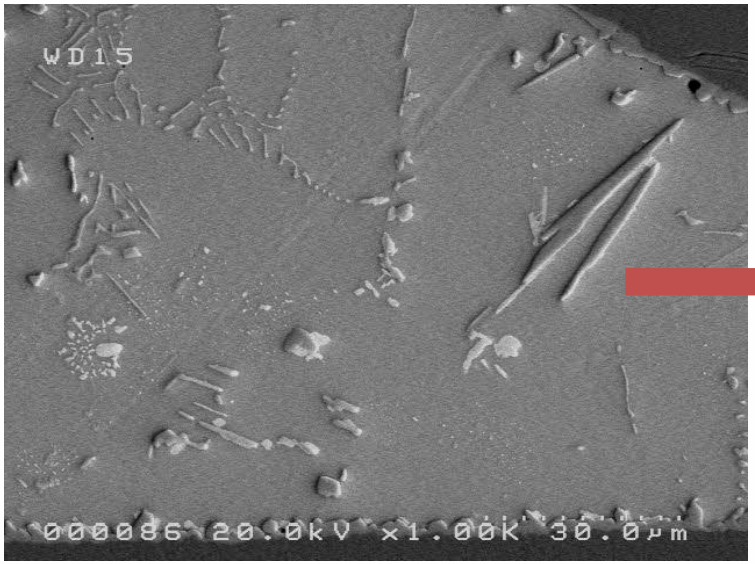

Cross Section showing Violet microstructure after assembly

3010 cycles ATC

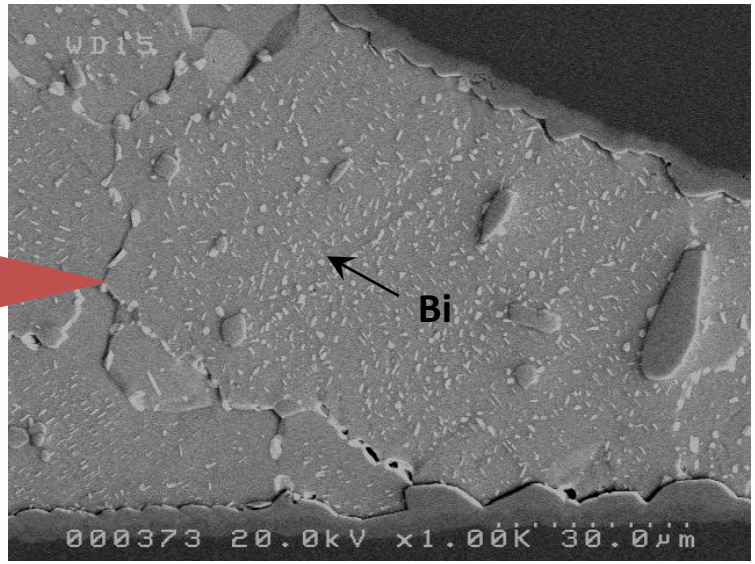

Cross Section showing Violet microstructure after 3010 cycles of harsh environment ATC

ATC Results and Analysis after 3010 cycles at -58° C to 130° C

Bi containing lead free alloys show improved microstructure after Harsh Environment Accelerated Thermal Cycling – definite improvement compared to SnPb solder exposed to the same conditions

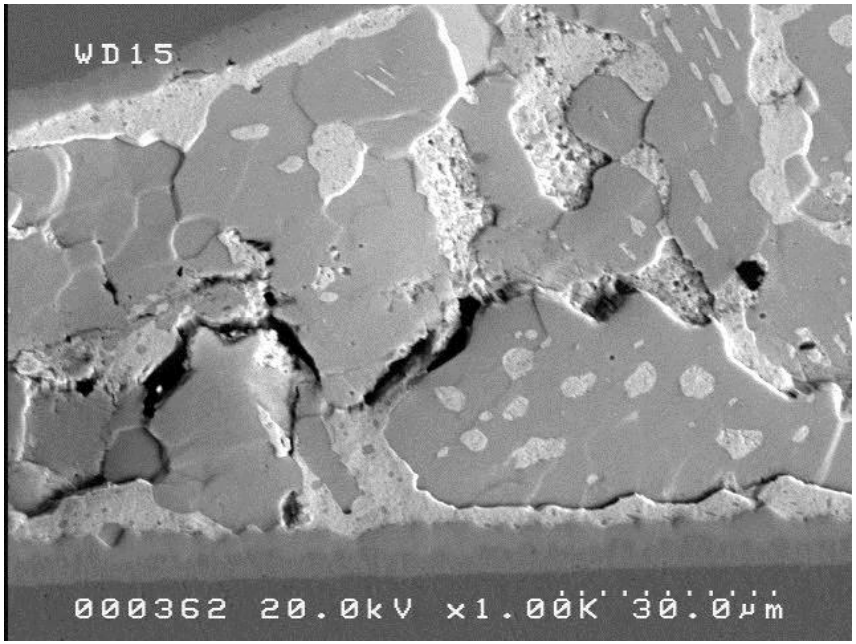

Cross Section showing SnPb microstructure after 3010 cycles of harsh environment ATC

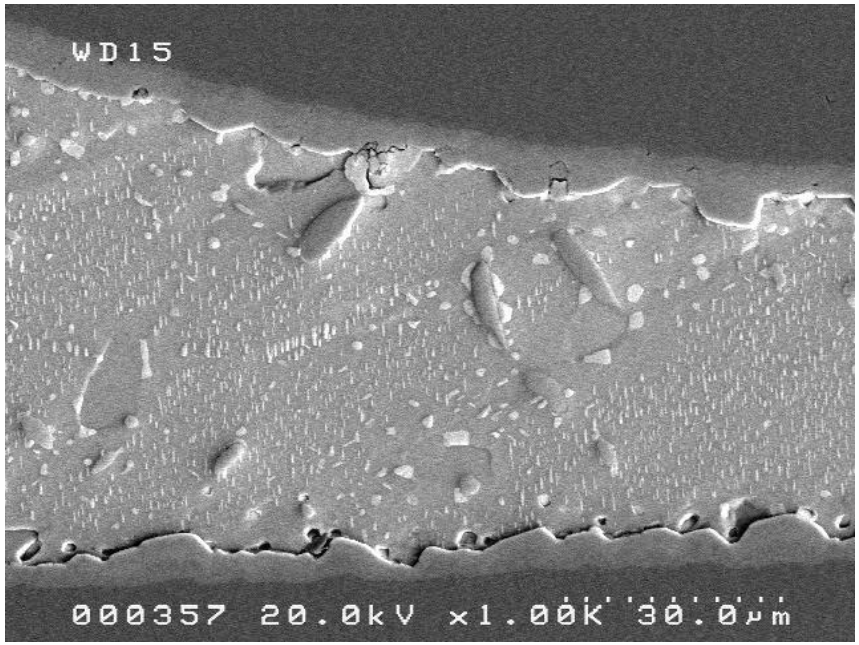

Cross Section showing Orchid microstructure after 3010 cycles of harsh environment ATC

Vibration Testing

- 26 test vehicles tested
  - 17 boards @ 5G vibration
  - 9 boards @ 2G vibration
- Boards further separated into groups; each group included different combinations of alloys, finishes and laminate
- Vibration was monitored along with resistance and strain data

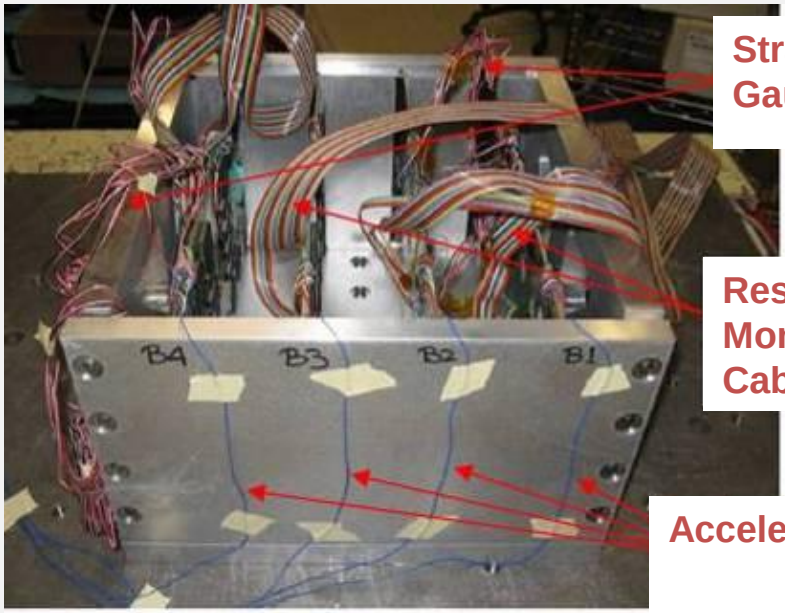

Vibration Fixture with Boards, monitoring systems shown

Vibration: Test Procedure and Techniques

1. Fixture Survey
   - Completed to ensure no resonance occurred within the test frequency

2. Sine Sweep Vibration
   - Frequency Range: 10 - 200Hz
   - G levels: 2G & 5G
   - Completed to find test vehicles resonance frequencies

3. Sine Dwell Vibration
   - Each batch subjected to a 6 hour (~1M cycles) sine dwell vibration at the closest common resonance frequency of the group.

The response G level on each board was measured using accelerometers

The response G level on each board was measured using accelerometers

Vibration: Strain Monitoring

- Two configurations of strain gauge attachments.
  - 2 rectangular rosette & 6 single axis strain gauges used on each board
  - rectangular rosette strain gauges used on BGA locations, uniaxial strain gauges on remaining component locations
  - 12 channels were monitored using the Vishay Measurement System

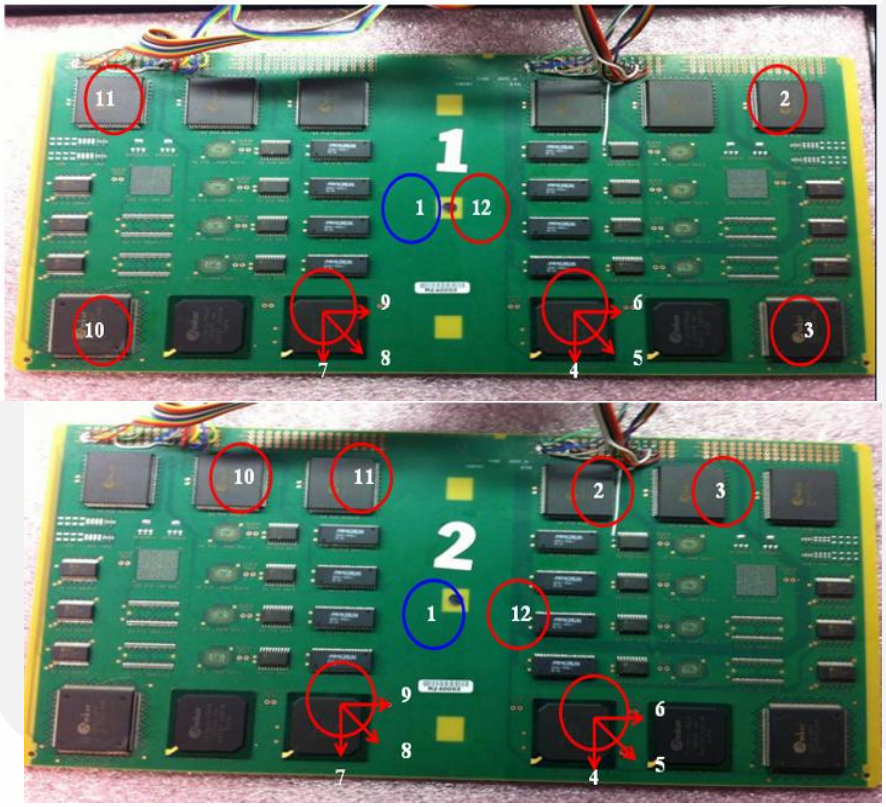

Strain Gauge Locations, Two Scenarios Shown (1 and 2)

Strain measurements were taken for all 2G & 5G sweeps. Also, strain was only recorded for first 5 minutes of every hour in the 6 hour dwell

Vibration: Resistance Monitoring

- Resistance was monitored on all 26 test vehicles, and 16 components were monitored on each.
- The **Anatech Event Detector** data collection was set up with a cycle time of 20 seconds, a data collection rate of every 2 seconds, and the data collection duration was the full testing time.
- Every two seconds, the system compared the collected value to the threshold value of 300 Ω

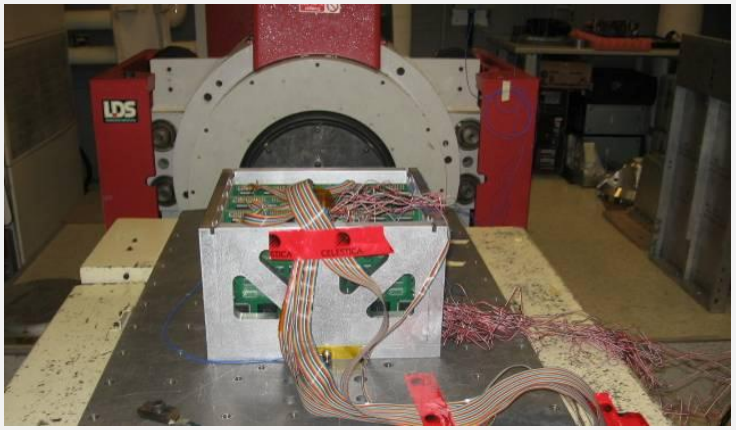

Vibration Fixture with Boards Mounted on Table with all Monitoring Systems

Resistance Monitoring System (Anatech Event Detector)

Technique for Vibration Testing

- For all samples, the 1st mode average resonance frequency was 52Hz as revealed via sine sweep vibrations.
- With input G level of 5G, the geometrical centre of the board experienced an average 55G at resonance.
- Resonance displacement amplitude p-p 10.2mm. Component solder failure occurred during this large bending momentum as a result of the high displacement.
- Average G level at resonance frequencies were 55G and 35G during the 5G and 2G sweeps, respectively

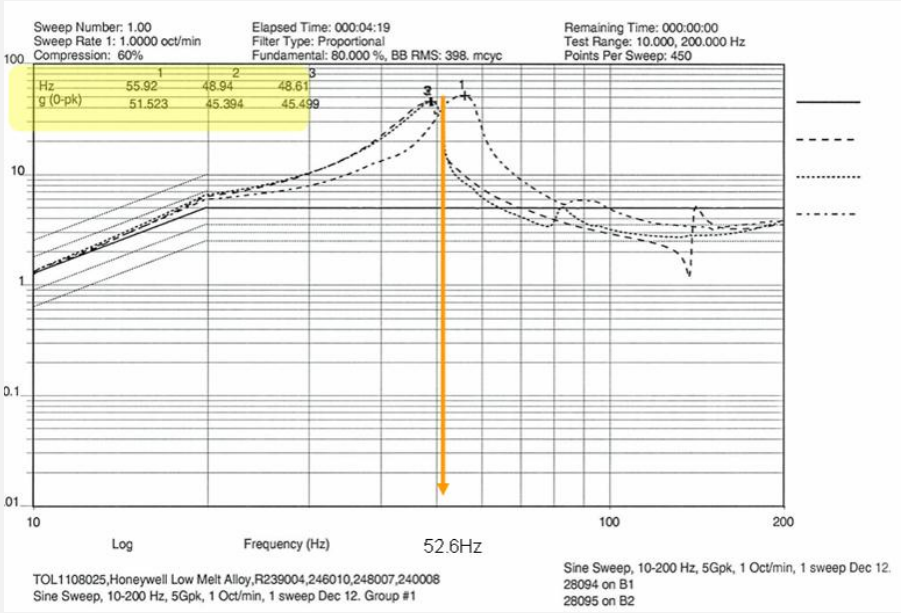

Technique for Vibration Testing

- Test results confirm that maximum strain occurs at resonance frequencies.
- Strain values are at a maximum in the center of the board and decrease in a non-linear pattern as the measurement point moves away from the center.
- Also, it was noticed that component strain values follow a steep downward pattern from the start of the test to just before the two hour mark. From here, strain values remain fairly consistent.

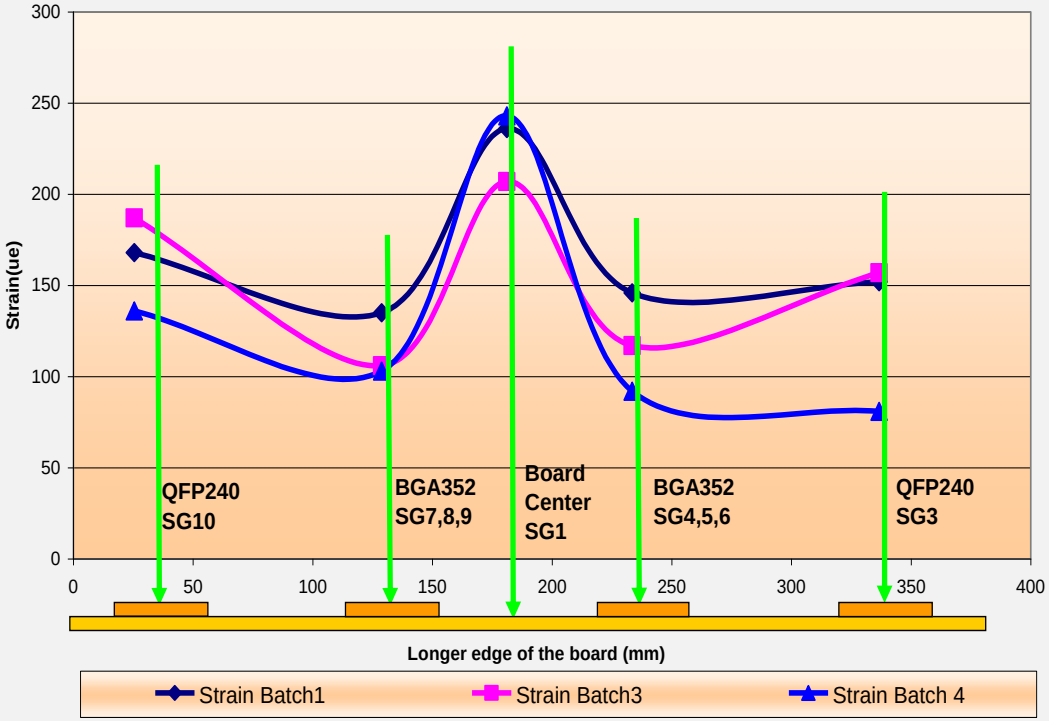

Vibration Resistance Measurements Analysis

Failures after 1M cycles for the screening experiment at 5G

Card #	R239008	R239004	R239009	R246002	R246006	R246010	R247002	R247007	R247010
Paste type	Paul			Violet			Orchid		
Finish	OSP	ENIG	ENEPIG	OSP	ENIG	ENEPIG	OSP	ENIG	ENEPIG
T_g	155	170	170	170	155	170	170	170	155
352 BGA	02/02	02/02	01/02	00/02	02/02	02/02	02/02	02/02	01/02
240 QFP	02/02	02/02	02/02	00/02	02/02	02/02	02/02	02/02	02/02
SSOP 48	00/06	02/06	00/06	00/06	00/06	00/06	01/06	02/06	00/06
PLCC 84	01/06	04/06	00/06	00/06	01/06	05/06	01/06	02/06	04/06

Card #	R248005	R248002	R248009	R248007	R240006	R240002	R240010	R240008
Paste type	SAC305				SnPb			
Finish	OSP	OSP	ENEPIG	ENEPIG	OSP	OSP	ENEPIG	ENEPIG
T_g	155	170	155	170	155	170	155	170
352 BGA	02/02	02/02	02/02	02/02	00/02	02/02	00/02	02/02
240 QFP	02/02	02/02	02/02	02/02	00/02	02/02	02/02	02/02
SSOP 48	00/06	01/06	00/06	00/06	00/06	00/06	00/06	00/06
PLCC 84	03/06	04/06	04/06	03/06	00/06	03/06	04/06	06/06

Vibration Resistance Measurements Analysis

3D Scatterplot of PLCC84 2^3 vs Paste vs Finish

Factorial with SAC305 & SnPb

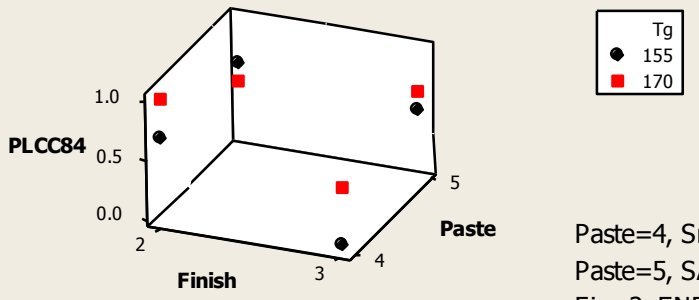

3D Scatterplot of 352BGA 2^3 vs Paste vs Finish

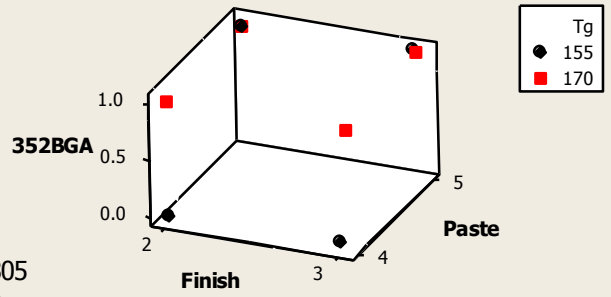

Paste=4, SnPb
Paste=5, SAC305
Fin=2, ENEPIG
Fin=3, OSP

3D Scatterplot of 240QFP vs Paste vs Finish

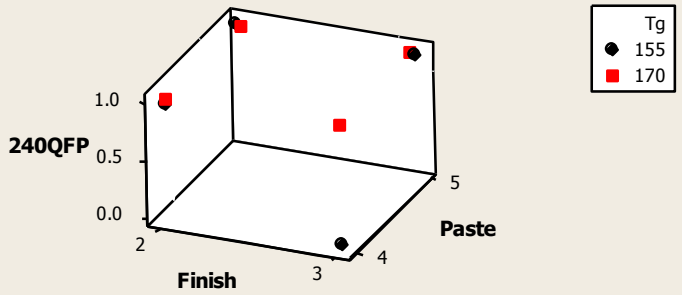

3D Scatterplot of SSOP48 vs Paste vs Finish

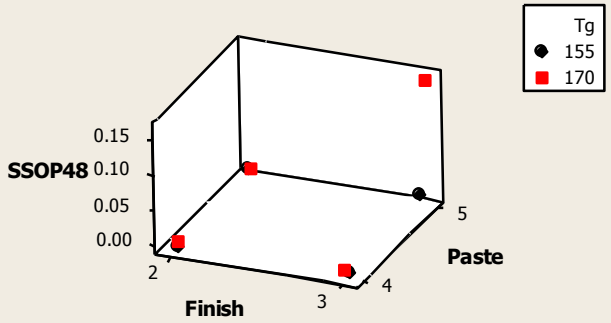

Vibration Resistance Measurements Analysis

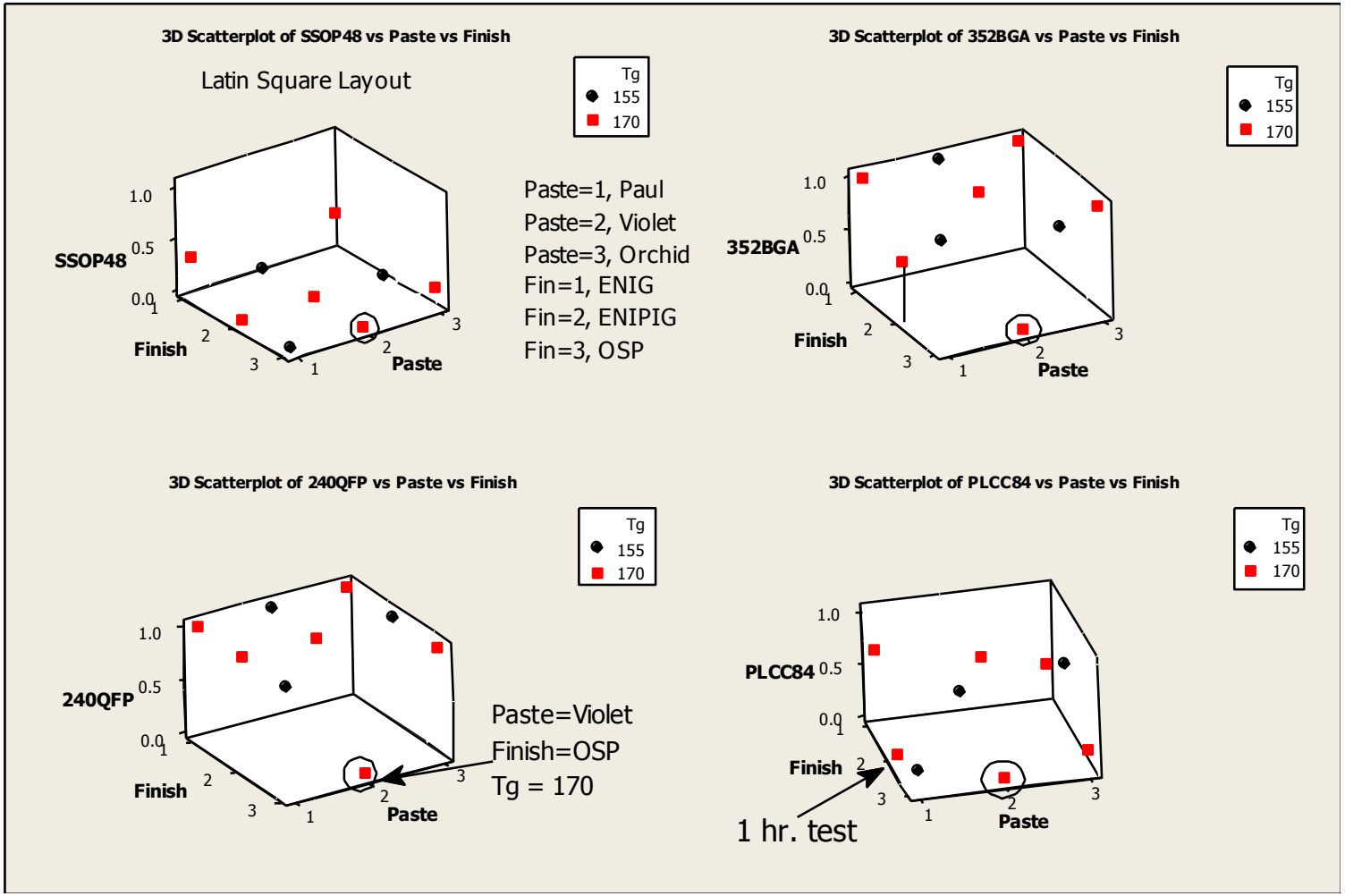

Vibration Resistance Measurements Details

Same failure trend between 2G and 5G with Violet, Paul, and Orchid

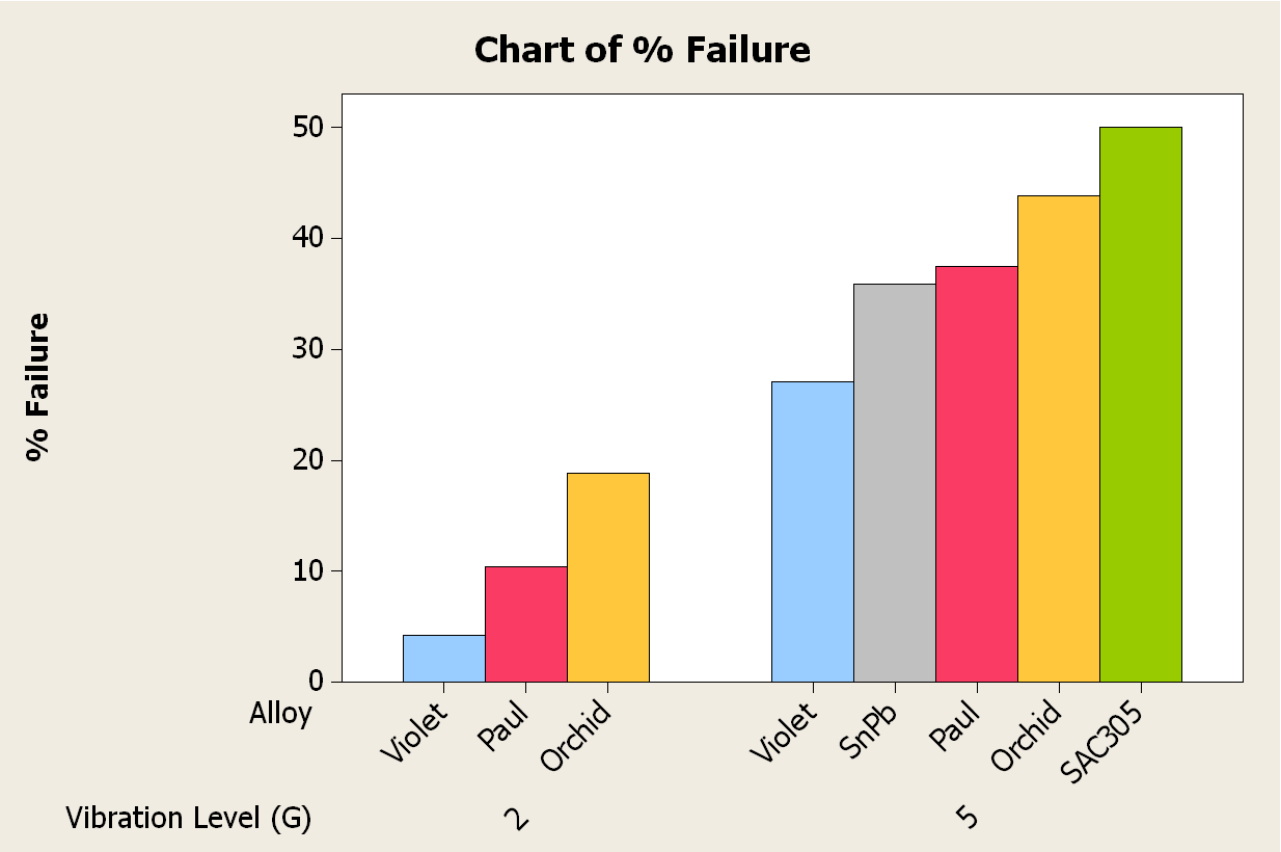

Vibration: Metallurgical Analysis

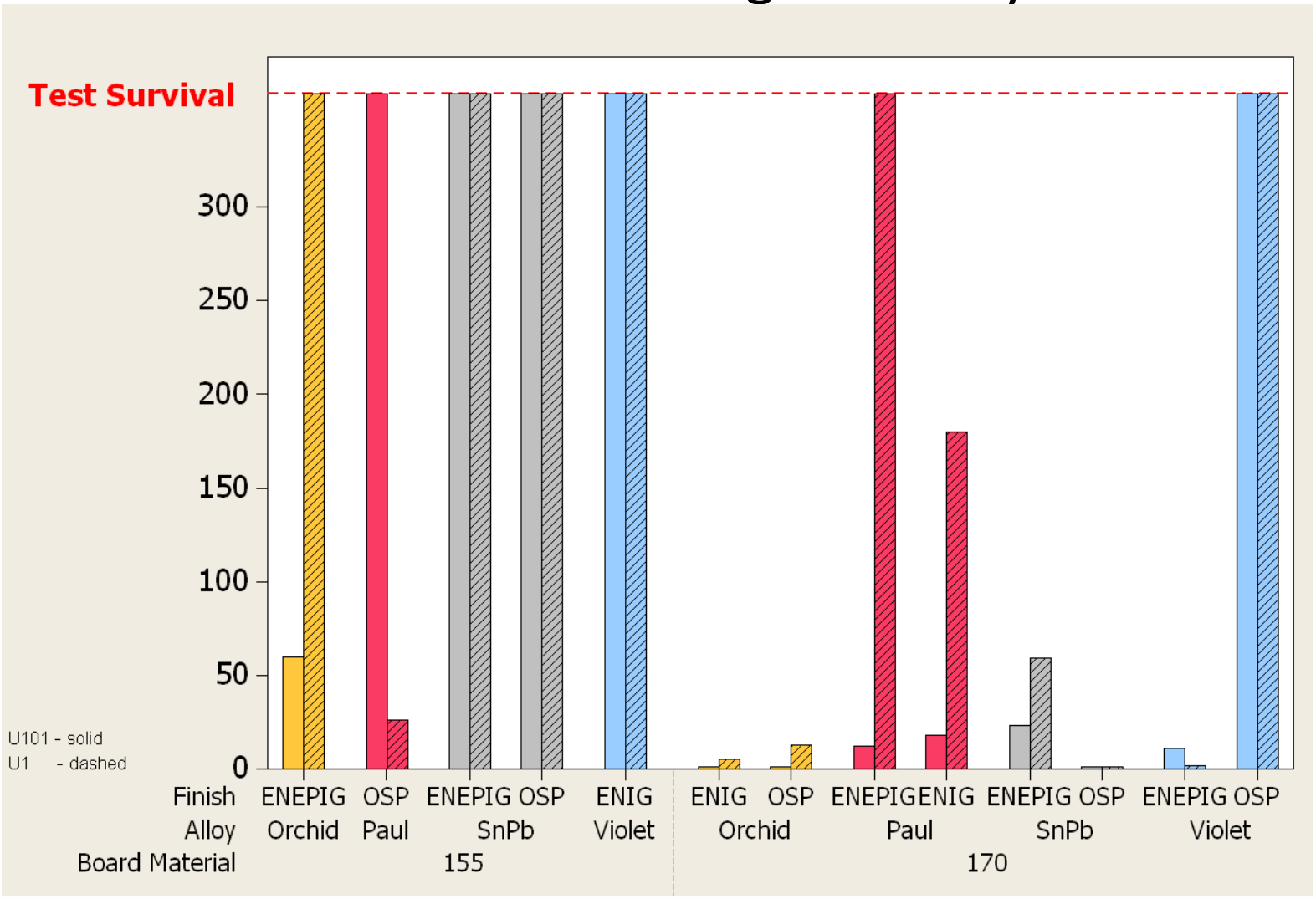

Vibration: Failures in 155°C T_g Boards after 5G

Board	155°C T_g					
Alloy	Violet	SnPb		Orchid	SAC305	
Surface Finish	ENIG	ENEPIG	OSP	ENEPIG	ENEPIG	OSP
Failure Mode	**No failure** - partial cracks near component and board side IMC	**No failure**	**No failure**	- pad cratering leading to damage of copper pad - fracture near component side IMC - fracture between IMC and copper pad	- fracture near component and board side IMC	-pad cratering leading to copper pad damage -fracture near component and board side IMC - barrel crack within via

Vibration: Failures in 155°C T_g Boards after 5G

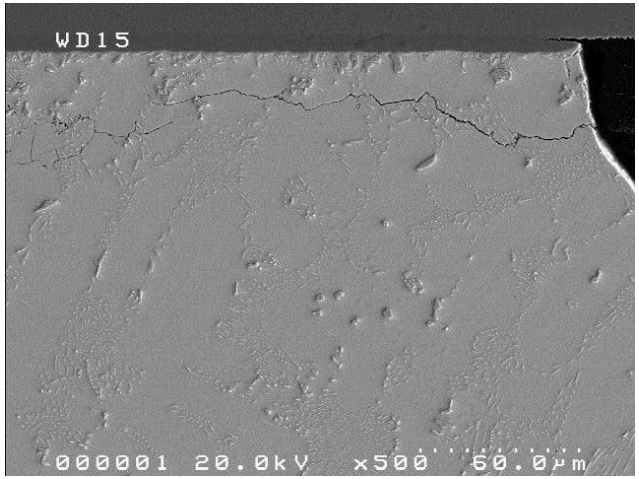

Partial fracture near component side IMC on BGA of Violet and SAC305 with an ENIG finish, 155°C T_g board

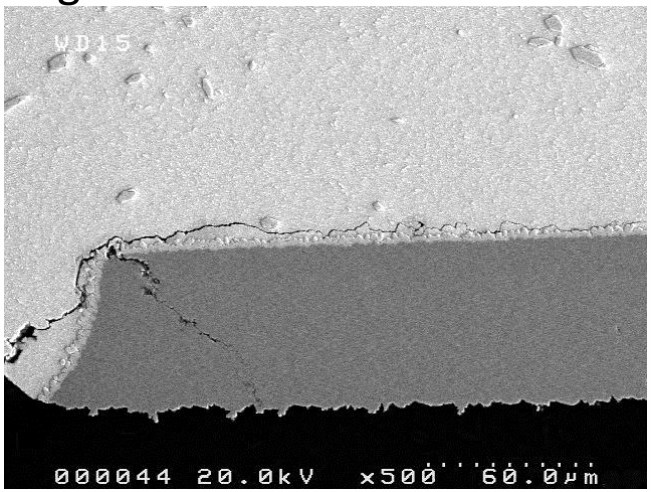

Fracture near board side IMC on BGA of SAC305 with an OSP finish, 155°C T_g board

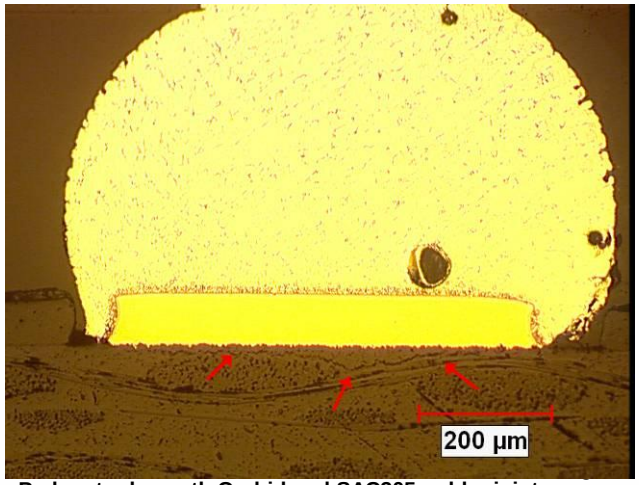

Pad crater beneath Orchid and SAC305 solder joint on ENEPIG finish, 155°C T_g board

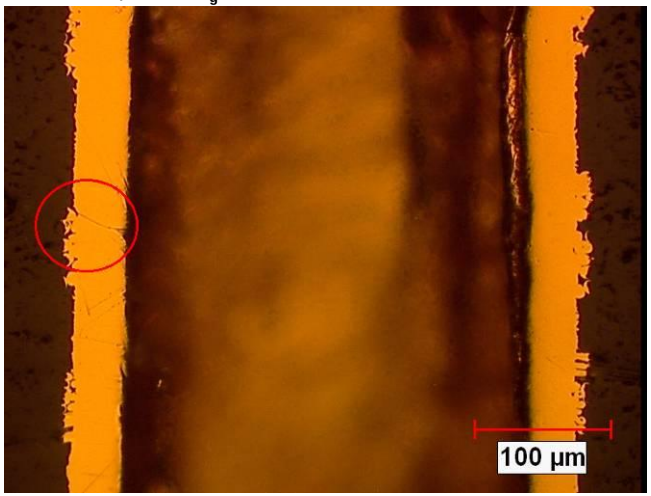

Barrel Crack in Via beneath SAC305 solder joint on OSP finish, 155°C T_g board

Vibration: Failures in 170°C T_g Boards after 5G

Board	170°C T_g							
Alloy	Violet		SnPb	Paul	Orchid		SAC305	
Surface Finish	ENEPIG	OSP	ENEPIG	ENIG	ENIG	OSP	ENEPIG	OSP
Failure Mode	- pad cratering leading to copper pad damage - fracture near component and board side IMC	**No failure**	- pad cratering leading to copper pad damage - fracture near component side IMC	- fracture near component and board side IMC - fracture between IMC and copper pad	- pad cratering leading to copper pad damage - fracture between IMC and copper pad	- fracture between IMC and copper pad	- pad cratering leading to copper pad damage - fracture near component and board side IMC	- pad cratering leading to copper pad damage - fracture near component and board side IMC

Vibration: Failures in 170°C T_g Boards after 5G

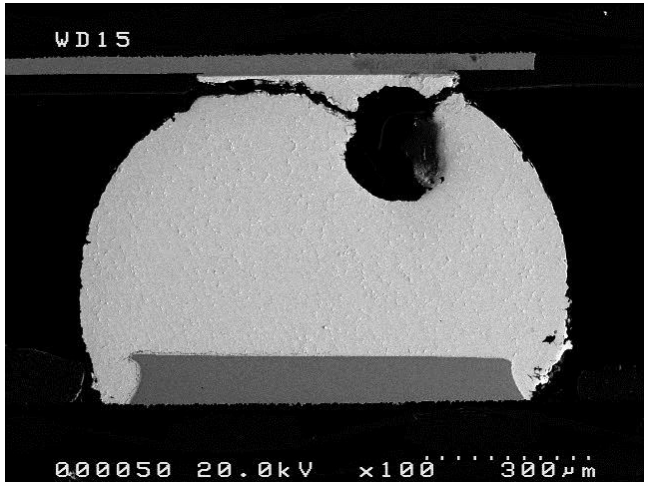

Complete fracture near component side IMC on BGA of SAC305 with an ENEPIG finish, 170°C T_g board

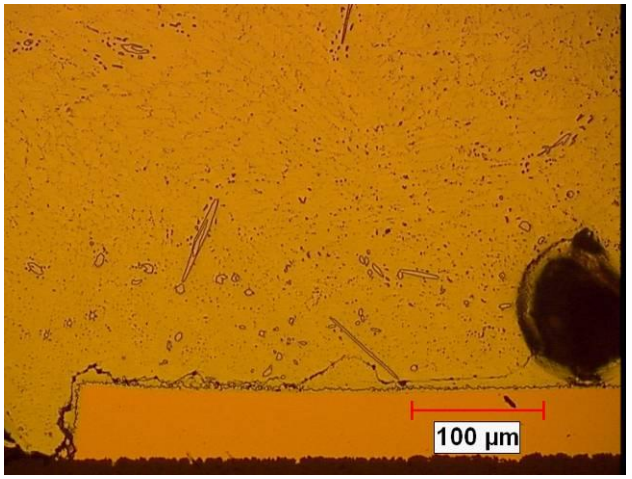

Fracture near board side IMC on BGA of SAC305 with an OSP finish, 170°C T_g board

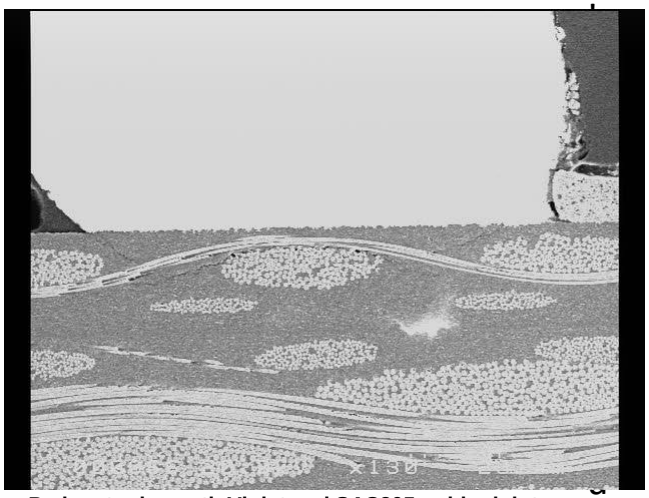

Pad crater beneath Violet and SAC305 solder joint on ENEPIG finish, 170°C T_g board

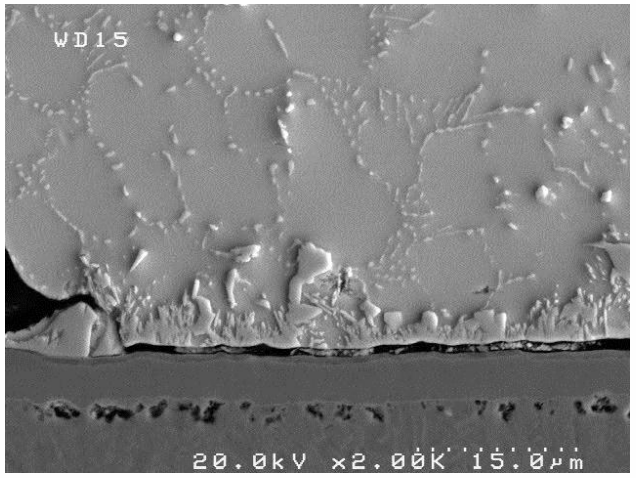

Fracture between IMC and copper pad of Paul and SAC305 solder joint on ENIG finish, 170°C T_g board

Vibration: Failure Analysis of QFPs

- QFPs failed at the leads
- The lead either broke at the knee or was ripped from the component
- No pad cratering occurred

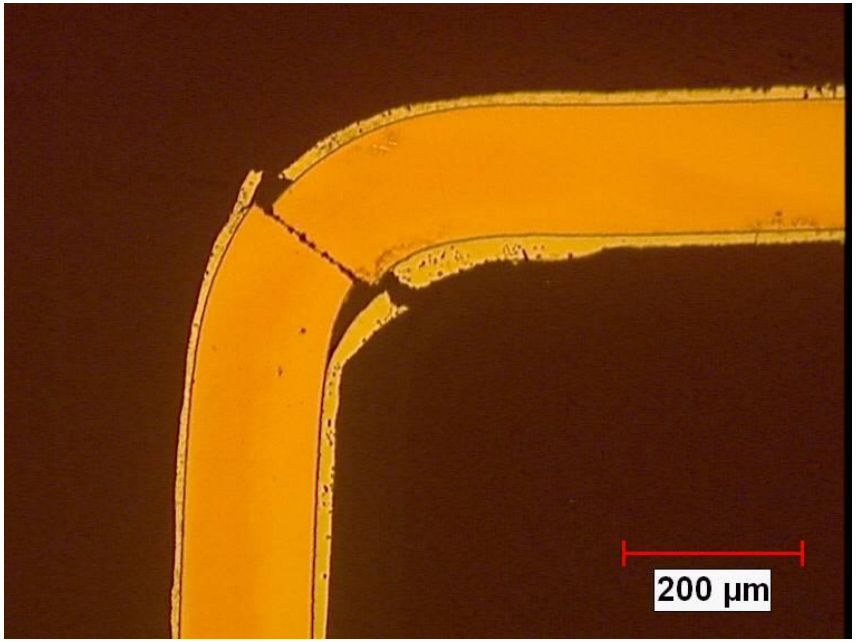

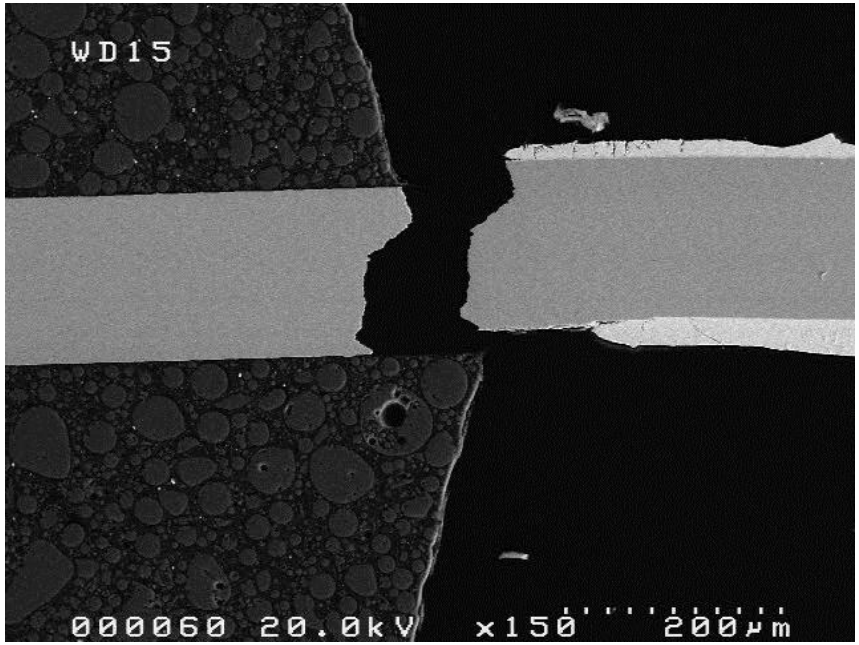

Vibration: Failure Analysis of QFPs

- Cracks were seen to form within the solder and propagate to the lead material
- Therefore, this QFP lead failures showed some alloy dependence in vibration testing
- Only Violet and SnPb solder joints survived completely after vibration testing

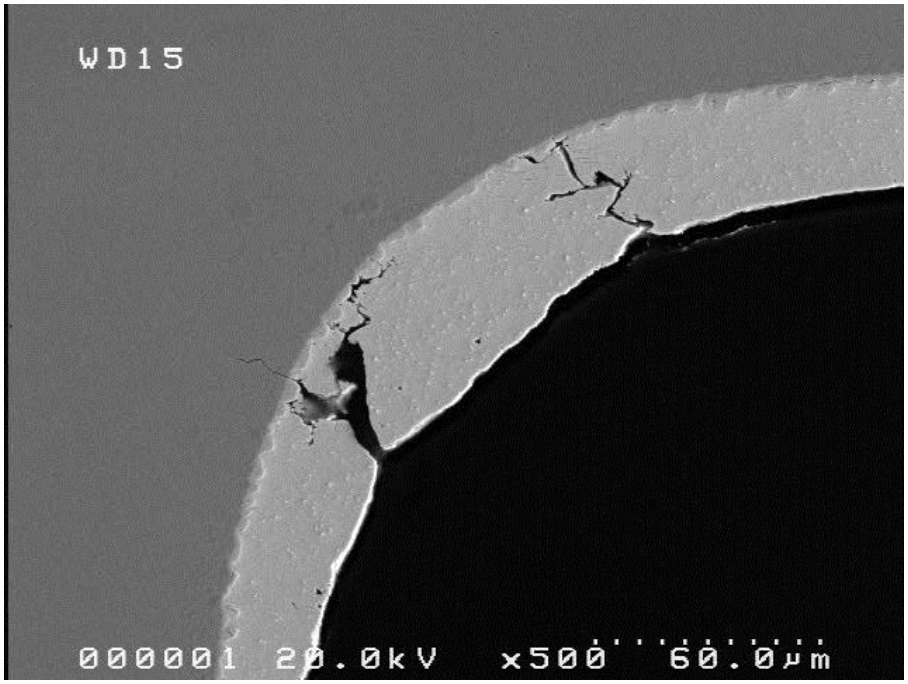

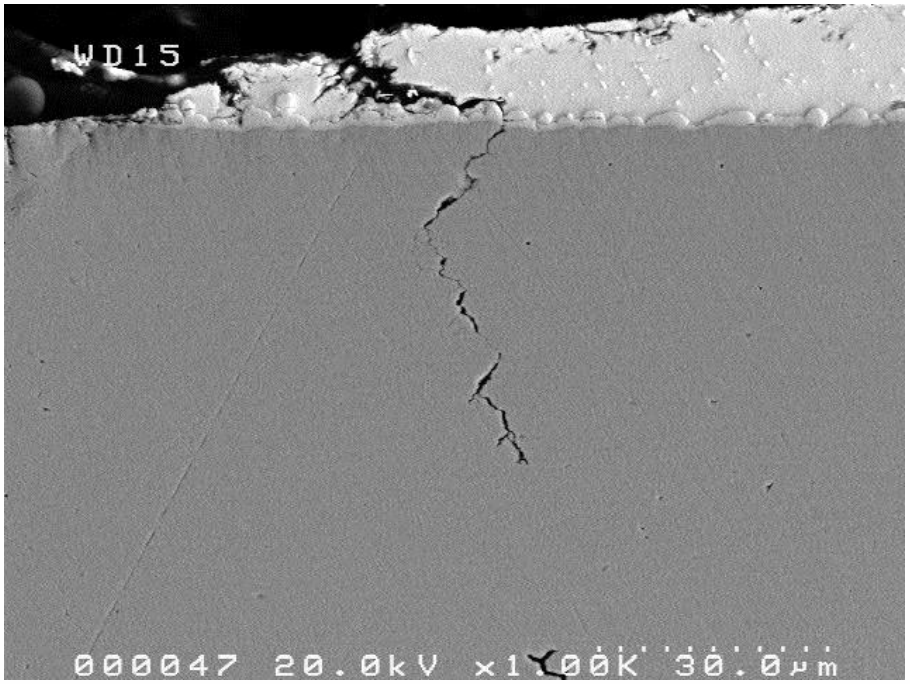

Summary and Conclusions

Screening experiments on the manufacturability and reliability of the lower melting Pb-free alloys that may satisfy the Aerospace requirements allow to make the following summary and conclusions.

- Three Bi-containing alloys: Sn3.4Ag4.8Bi (Paul) and two reduced Ag content variations, with and without Cu, Sn2.25Ag0.5Cu6Bi (Violet) and Sn2Ag 7Bi (Orchid), were selected.
- Honeywell test vehicles were assembled using these alloys with the process temperature about 10° C below SAC305.
- Two board materials with high Tg and normal Tg were used. The boards were finished with OSP, ENIG, and ENEPIG.

No problems related to the manufacturability were detected. Experimental alloys had better wetting and less voiding than SAC305. The joints had a proper shape comparable to both SnPb and SAC305.

Summary and Conclusions: Microstructural Analysis

- Sn3.4Ag4.8Bi (Paul) and Sn2Ag 7Bi (Orchid) are not fully compatible with ENIG and ENEPIG, forming irregular and/or thicker interfacial intermetallic than SAC305. This is attributed to the lack of Cu in these alloy compositions
- The alloy with Cu, Sn2.25Ag0.5Cu6Bi (Violet), is compatible not only with OSP, but also with ENIG and ENEPIG, and forms excellent solder joints with uniform intermetallic layers on both ball grid array and leaded components
- On the ENEPIG finish, Pd-containing needle-shaped intermetallic particles are present in solder joints. These particles may cause solder joint embrittlement. The ENEPIG finish must be fully qualified for Aerospace industry acceptance

All three Bi-containing alloys formed excellent joints on OSP finish. The interfacial intermetallic layer is comparable to SnPb in thickness and shape and thinner than in SAC305

Summary and Conclusions: ATC

- All combinations of alloys (Paul, Violet, Orchid, SAC305 and SnPb), surface finishes (OSP, ENIG and ENEPIG) and board laminate (normal and high Tg) passed the aerospace ATC qualification requirement of 1000 cycles of -55° C to 125° C. There was no solder joint failure on both high and normal Tg boards up to 3010 cycles for Pb-free lower melt and SAC305 alloys.

- However, there were via failures in normal Tg boards with OSP finish, assembled using all Pb-free and SnPb solders. Of these via failures on normal T_g OSP-finished boards, only the SAC305 cell did not meet the aerospace qualification requirement of 1000 cycles.

- An exceptional influence of bismuth additions on microstructural changes during thermal cycling was observed. Bi particles evenly precipitate in the tin matrix and reduce microstructure degradation.

Therefore, all three experimental alloys Paul, Violet, and Orchid showed excellent performance in harsh environment thermal cycling.

Summary and Conclusions: Vibration

- The vibration failure results are based on one million cycles and show failure modes that might give an indication of what material combinations fail early. These observations for high reliability products are important benchmarks. Both 2G and 5G vibration levels showed a similar failure progression of the number of failures based on resistance measurements. The order of the failure stays the same.

- Our recommendation for future work would be to start at 5G and then to select the higher G level that would precipitate more representative failure modes for the given amount of test time.

- The lowest failure rate found was for Violet followed by Paul and Orchid at the 2 G level. Violet and Paul showed the lowest rate of failure at the 5G level, followed by SnPb and Orchid. The SAC305 had the highest failure rate.

Violet and Paul responded more like SnPb than SAC305, and thus appear to be a consistent, lower melt, robust substitute for SnPb.

Summary and Conclusions: Vibration

- The failure mode of QFPs in vibration testing was full cracking of the copper leads, which were observed to have initiated in the solder that wicked up along the lead during reflow.
- BGAs failed in vibration most frequently due to cracking through the bulk solder and laminate material creating some degree of pad cratering. The cracks from the laminate material may propagate through the copper pad to the solder material, resulting in open joints.
- The 155° C T_g laminate material demonstrated a trend to pad cratering reduction compare to the 170° C T_g material.
- Both ENIG and ENEPIG finishes showed failures at the IMC; ENEPIG exhibited failure through the brittle IMC formed with Orchid solder pastes, whereas ENIG resulted in failure between the IMC and copper pad with all alloys.

Summary and Conclusions

These screening experiments provide some insight into the main effects of the alloy performance and show positive evidence for future study. Based on the results of the screening experiments, the lower melting alloys containing bismuth, particularly Violet and Paul, are recommended for further statistically valid reliability testing. The recommended testing will enable the choice of an alternative RoHS Pb-free alloy with lower process temperature and better thermomechanical properties.

Future Work

- These screening test results will be shared to help launch a new NASA consortium phase 3 project focused on the requirements of the Aerospace industry. This work should provide some statistical data for deeper reliability analysis.
- Additional research for items like rework and combined environmental testing should be completed to continue the investigation of the alloy for extended manufacturing practices.
- Considerations for work using this alloy on product trials should be evaluated for an aerospace non-critical product of interest to demonstrate the alloy performance.

Acknowledgements

The authors would like to thank the following individuals from Celestica: Russell Brush, Alon Walk, Kangwon Lee, Veseyathaas Thambipillai for ATC testing and data analysis; Jie Qian for sample preparation; Jose Traya and Michael Emery for test vehicle assembly; Michelle Le for vibration testing; and Dr. John Vic Grice, Honeywell Corporate consulting statistician, who helped design the experimental matrix.

BACKUP SLIDES

Wetting Properties

- SnPb has best wetting properties
- Paul, Violet and Orchid are improvements on SAC305

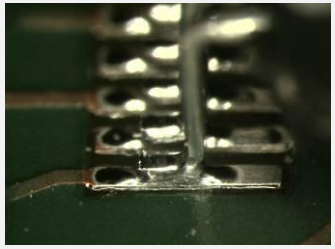
SnPb

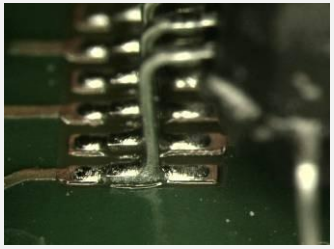
SAC305


Paul

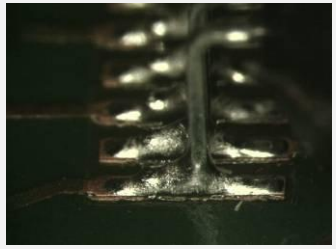
Violet

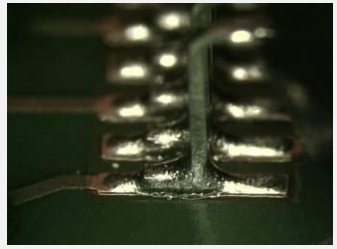
Orchid